INFRARED SYNCHROTRON RADIATION: FROM THE PRODUCTION TO THE USE

Stefano Lupi

Department of Physics
Sapienza University of Rome,
CNR-IOM, INFN and SISSI@Elettra (EU-Italy)

FREQUENCY AND TIME-RESOLVED
TERAHERTZ SPECTROSCOPY

Outline

- Production and Properties of Infrared Synchrotron Radiation;
- Experimental Apparatus: Michelson Interferometry+Infrared Microscopy
- Solid-State Applications:
  Superconduting Transition (THz and Far-IR Spectroscopy)
  Gap determination
  Spectral-Weight and penetration depth
  Metal-to-Insulator Transitions
- Biology:
  Cellular absoption and replication
- Geological Applications:
  Microscopic fluid inclusions
- Chemistry:
  Adbsorption at solid surfaces
- New developments
  THz non linear Spectroscopy
  Go beyond the diffraction limit: Infrared Nanoscopy

Electromagnetic Spectrum

The "THz gap", Collective Excitations in Macromolecules and exotic electronic materials

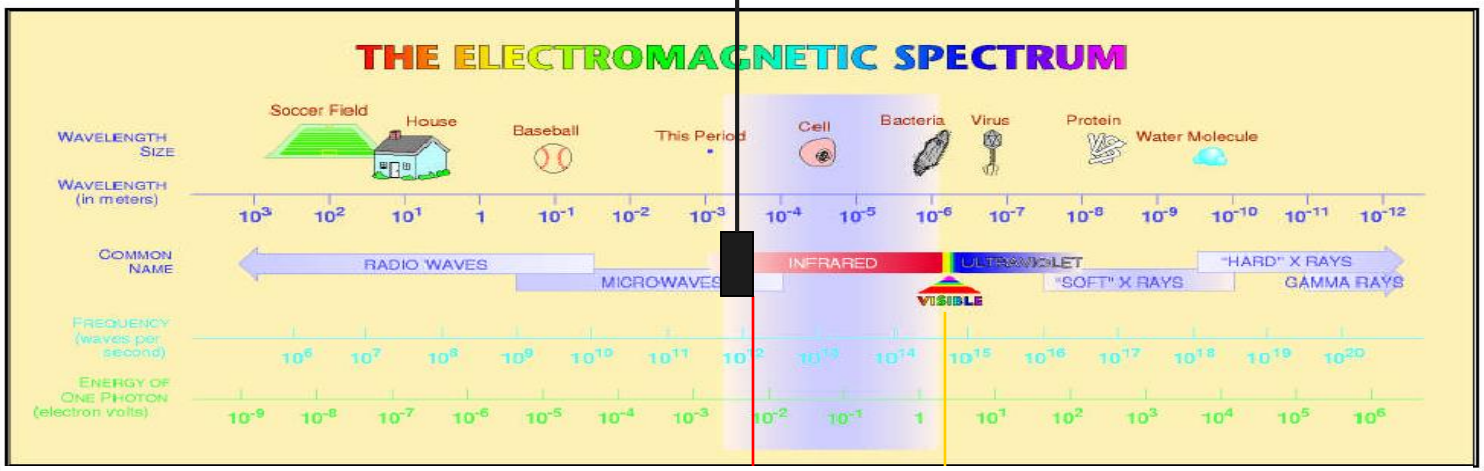

IR Units: 200 cm^{-1}=300 K= 25 meV = 50 μm = 7 THz

FIR MIR NIR

Phonons;
Drude absorption;
Gaps in superconductors;
Molecular Rotations;

Molecular Vibrations
Fingerprints for
Chemistry, Biology,
And Geology

Molecular Overtones and
Combinations bands;
Excitons;
Gaps in semiconductors

Infrared History

Volume 1. *July–August, 1893.* *Number 1.*

THE

PHYSICAL REVIEW.

A STUDY OF THE TRANSMISSION SPECTRA OF CERTAIN SUBSTANCES IN THE INFRA-RED.

By Ernest F. Nichols.

WITHIN a few years the study of obscure radiation has been greatly advanced by systematic inquiry into the laws of dispersion of the infra-red rays by Langley,[1] Rubens,[2] Rubens and Snow,[3] and others. Along with this advancement has come the more extended study of absorption in this region. The absorption of atmospheric gases has been studied by Langley[1] and by Ångstrom.[4] Ångstrom[5] has made a study of the absorption of certain vapors in relation to the absorption of the same substances in the liquid state, and the absorption of a number of liquids and solids has been investigated by Rubens.[6]

In the present investigation, the object of which was to extend this line of research, the substances studied were: plate glass, hard rubber, quartz, lamp-black, cobalt glass, alcohol, chlorophyll, water, oxyhæmoglobin, potassium alum, ammonium alum, and ammonium-iron alum.

[1] Report on Mt. Whitney Expedition, Profess. Papers, U. S. Signal Service, XV.
[2] Annalen der Physik und Chemie, N. F. XLV., p. 238.
[3] Annalen der Physik und Chemie, N. F. XLVI., p. 529.
[4] Bihang till K. Svenska Vet.-Akad. Handlingar, Band 15, Afd. 1, No. 9.
[5] Ofversigt af Kongl. Vetenskaps-Academiens Forhandlingar, 1890, No. 7, Stockholm.
[6] Annalen der Physik und Chemie, N. F. XLV., p. 258.

~ 50 IRSR Beamlines in the World

1976	Meyer and Lagarde (LURE, Orsay) publish the first paper on IRSR
1981	Duncan and Yarwood observe at Daresbury the first IRSR emission
1985	The first IRSR spectrum (on N_2O) is collected at Bessy (Berlin)
1986	The first beamline becomes operating at UVSOR (Japan)
1987	Beamline at Brookhaven (USA)
1992-94	Beamlines at Orsay (France), Lund (Sweden), Daresbury (GB)
1995	First international workshop on IRSR, Rome (Italy)
2001	First IR beamline in Italy (SINBAD@DAΦNE)
2006	Second beamline in Italy (SISSI@Elettra)
2015	First THz beamline in Italy (TERASPARC@SPARC)
2017	Second THz beamline in Italy (TERAFERMI@Elettra)

Production of IRSR

Standard Bending radiation

(emitted during the circular trajectory in the bending due to the constant B field)

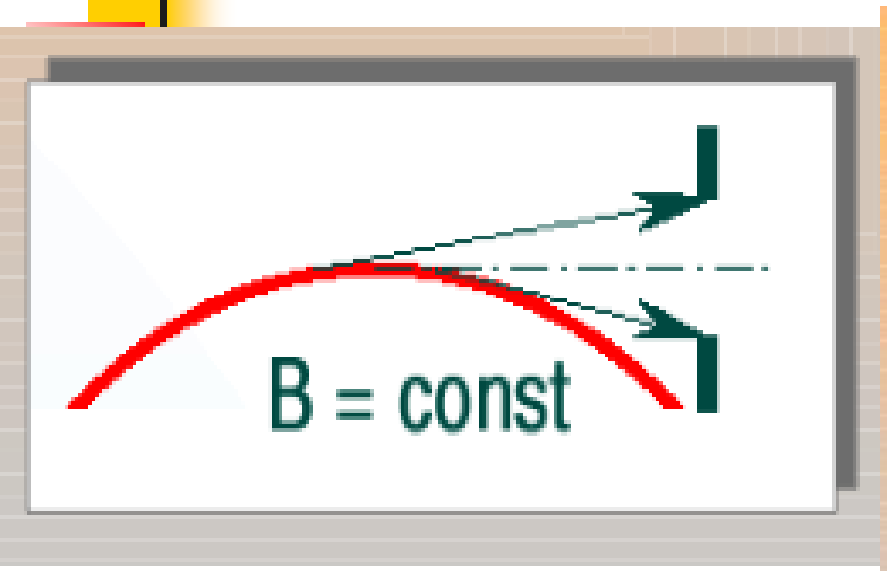

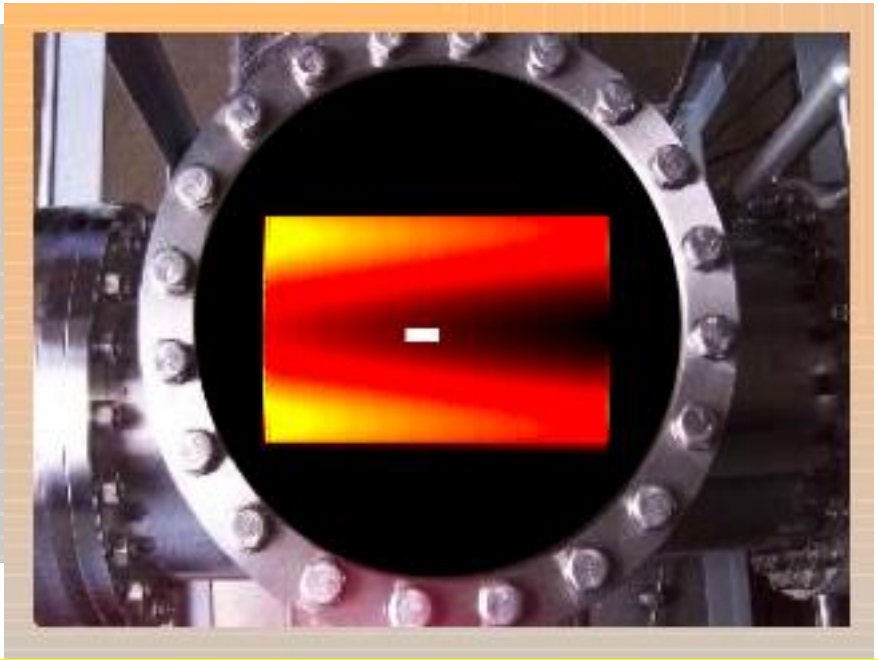

$$P(\lambda) = 4.4\ 10^{14} \times I \times \Theta_H \times bw \times (\rho/\lambda)^{1/3} \text{ photons s}^{-1}$$

I is the current in amperes,

Θ_H **(rads)** the horizontal collection angle,

bw the bandwidth in per cent, λ the wavelength, and ρ the radius of the bending

$$\Phi_{V\text{-}NAT}(\text{mrad}) = 1.66(1000 \times \lambda\ (\mu\text{m})/\ \rho(\text{m}))^{1/3}$$

at ALS for λ= 100 μm ➡ $\Phi_{V\text{-}NAT}$= 50 mrads

Very large emission angles
SISSI: H=70 mrads; V=25 mrads

Edge Emission

(emitted at the entrance (exit) of a bending magnet due to the rapid variation of the B field)

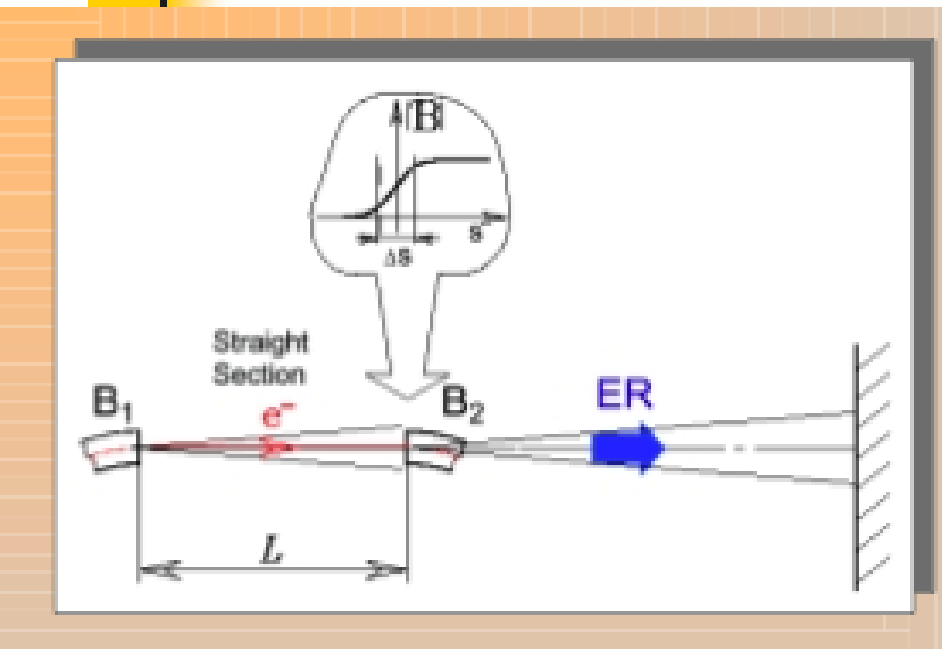

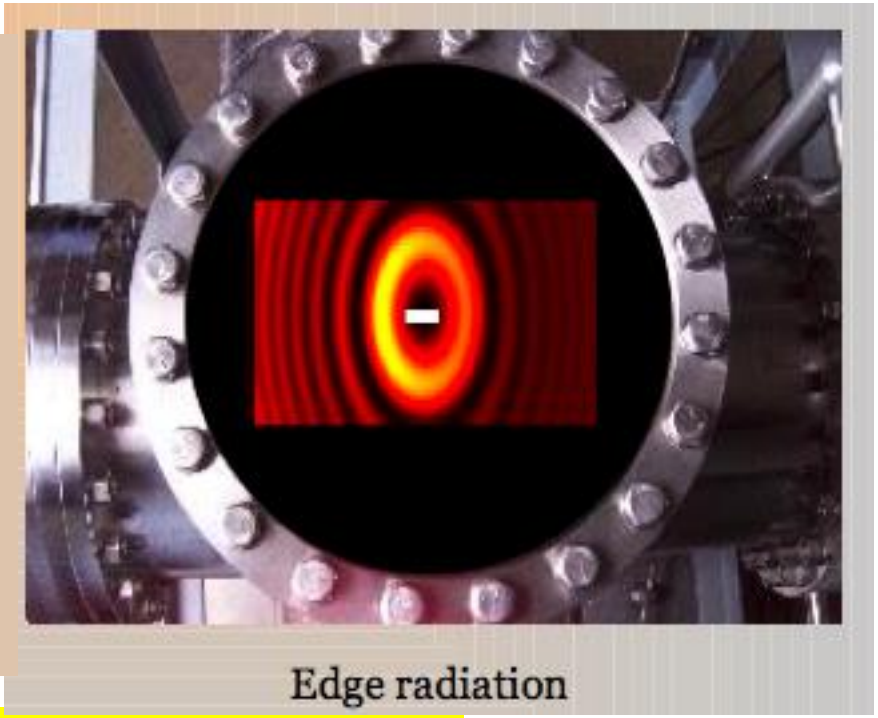

In the Far-Field approximation:

$$P = \alpha \times I \times \gamma^4\Theta^2/(1+\gamma^2\Theta^2)^2 \text{ photons s}^{-1}$$

I is the current in amperes,
Θ(rads) the emission angle
(concentrated in $\Theta_{max} \sim 1/\gamma \sim 10$ mrads)

IRSR FLUX

The IRSR flux and Brilliance depend only on:

-beam current
-source size/emittance
-extraction aperture
-transmission optics

Instead scarcely depend on the machine energy

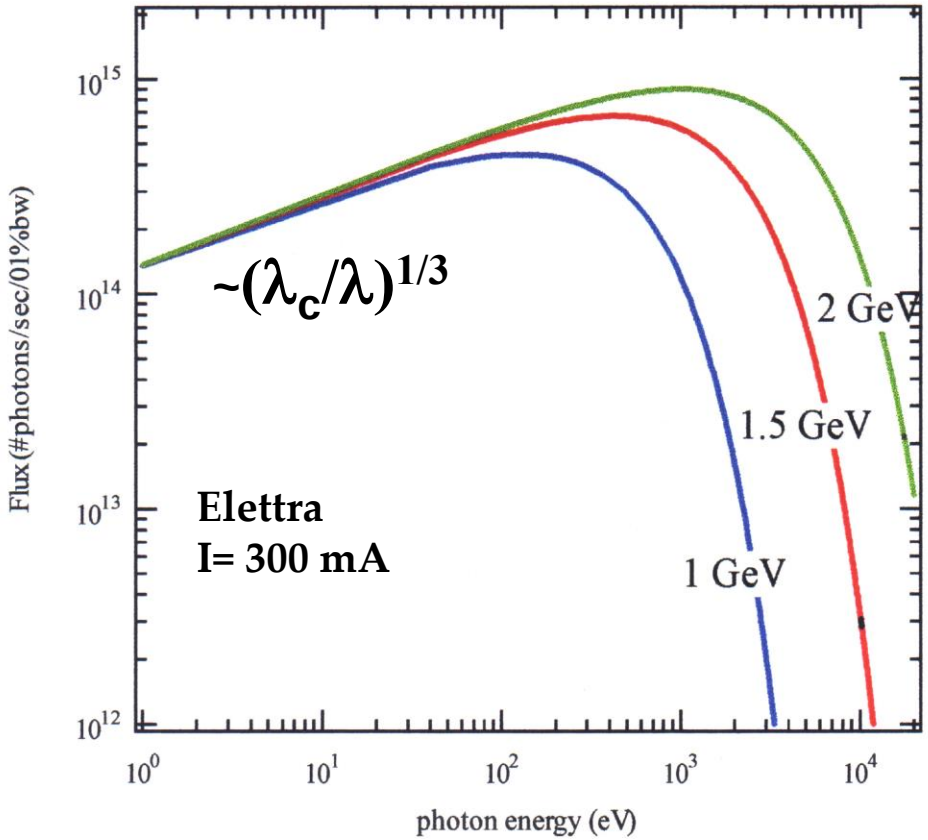

IRSR Brilliance

The most important figure of merit for IRSR is the **Brilliance**

$$B_{SR} = \frac{d^2F/d\theta d\varphi}{ASA}$$ (photons/0.1%bw/cm^2/str)

Where the **A**ctual **S**ource **A**rea is an estimation of the dimension of the source at the exit port (Hulbert and Weber,92; A. Nucara, 1998)

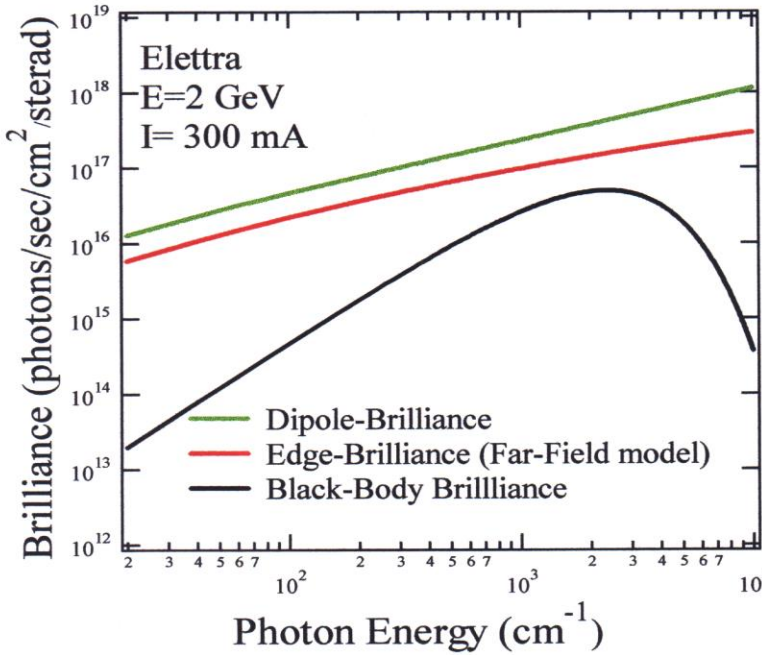

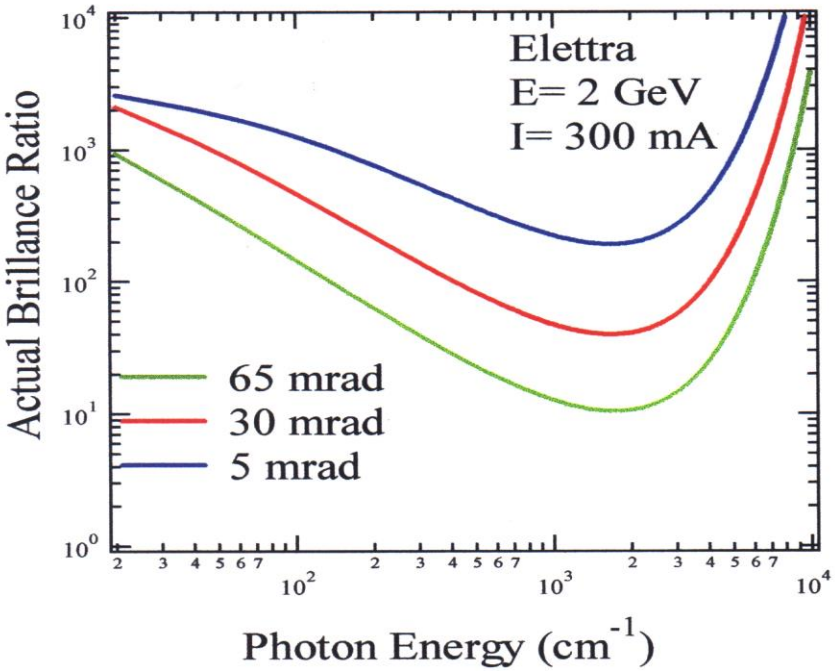

Limiting Noise

$$\%N = \frac{100A^{1/2}D^*}{B(\nu)\Delta\nu\varepsilon t^{1/2}\xi}$$

Where: A detector area, D* detectivity, **B brilliance**, Δν bandwidth, ε etendue, t measuring time, ξ optical efficiency

Advantages of IRSR

ADVANTAGES:

- FLUX GAIN
- BROAD BAND
- LINEAR & CIRCULAR POLARIZATION

→ SPECTROSCOPY

- BRILLIANCE GAIN
  - Diffraction Limited Spatial Resolution
  - Better Signal-to-Noise
  - Faster Data Collection

→ MICROSCOPY

SISSI (Source for Imaging and Spectroscopy in the Infrared)

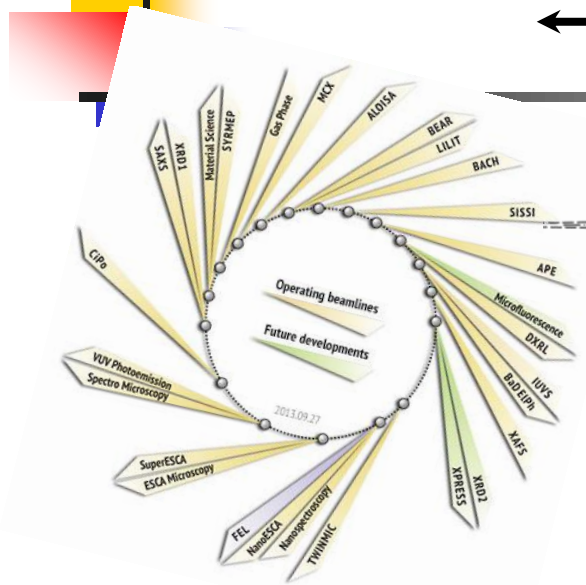

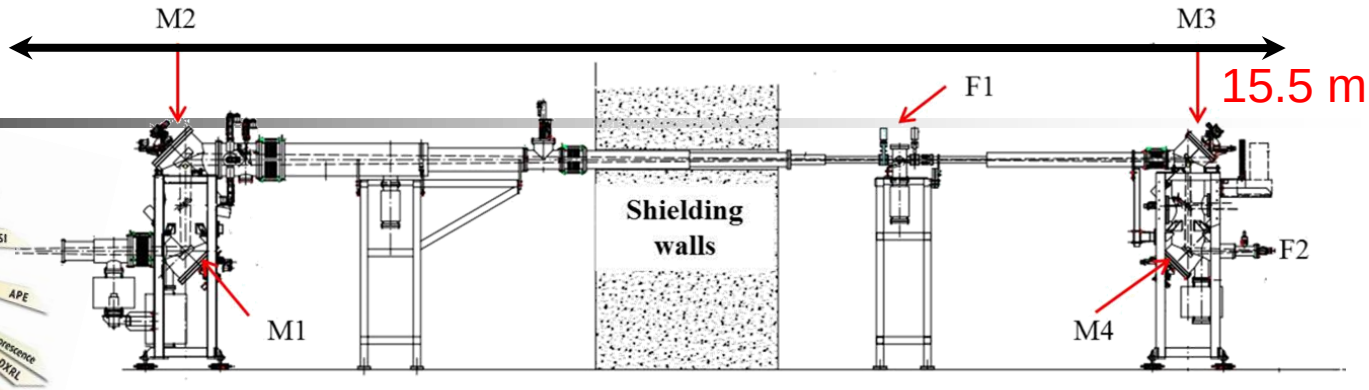

Elettra Sincrotrone Trieste

iom Istituto Officina dei Materiali

65±5 (H) x 25 (V) mrad

	Figure	Dimension HXV (cm^2)
M1	Plane	30X15
M2	Ellipsoidal	35X18
M3	Plane	15X8
M4	Ellipsoidal	16X10

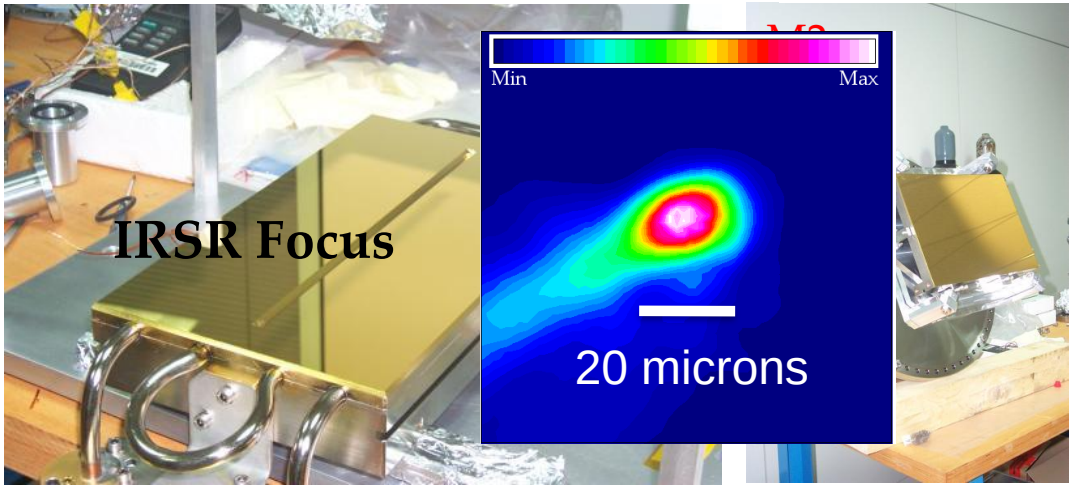

Brilliance gain at SISSI

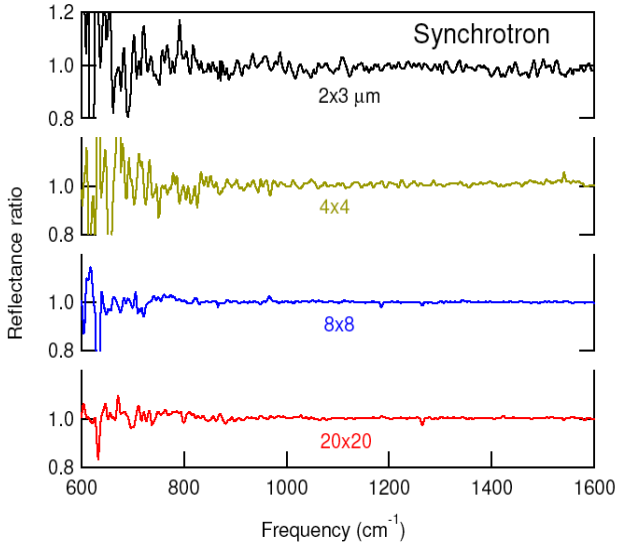

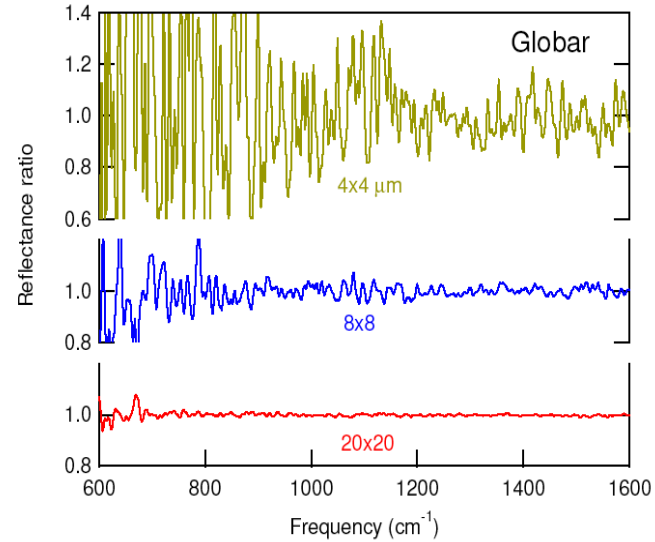

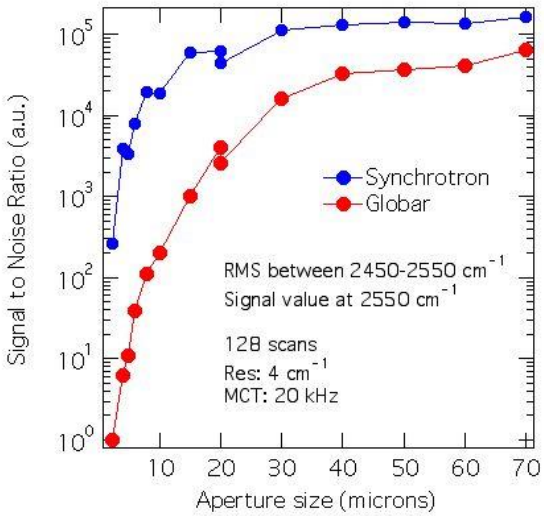

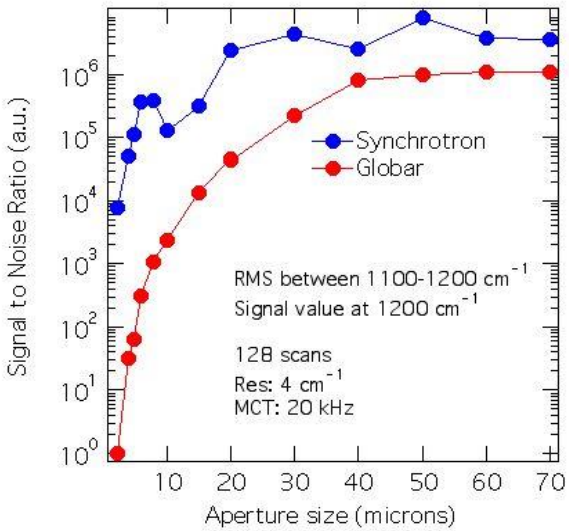

A.Perucchi, L.Vaccari, and S.Lupi, *Infrared Spectroscopy with Synchrotron Radiation*
In Synchrotron Radiation: Theory and Applications, Ed. S. Mobilio et al., (2015)

Increasing the Far-IR Flux: Coherent *vs* Incoherent Synchrotron Radiation

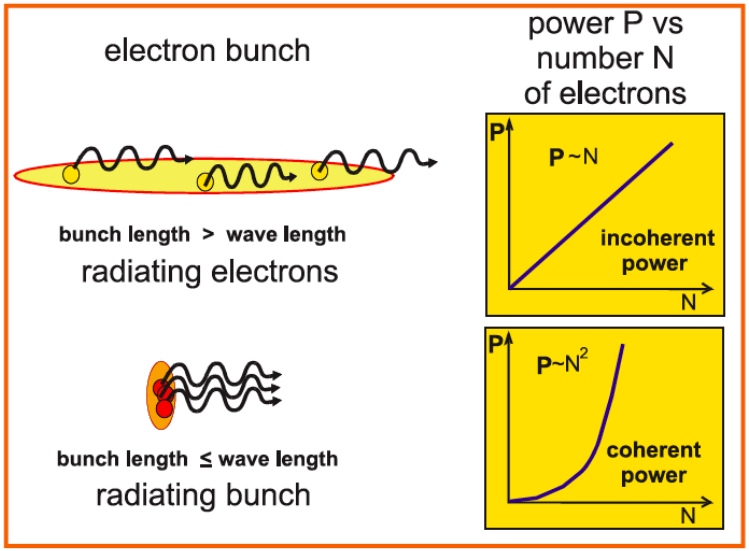

Flux:

$$I = I_{incoh} + I_{coh} = (N(1 - f_\nu) + N^2 f_\nu) I_{incoh}$$

$$f_\nu = \left| \int n(z) e^{i\pi \cos(\theta) z \nu} dz \right|^2$$ Bunch form factor

Diffraction due to chamber size

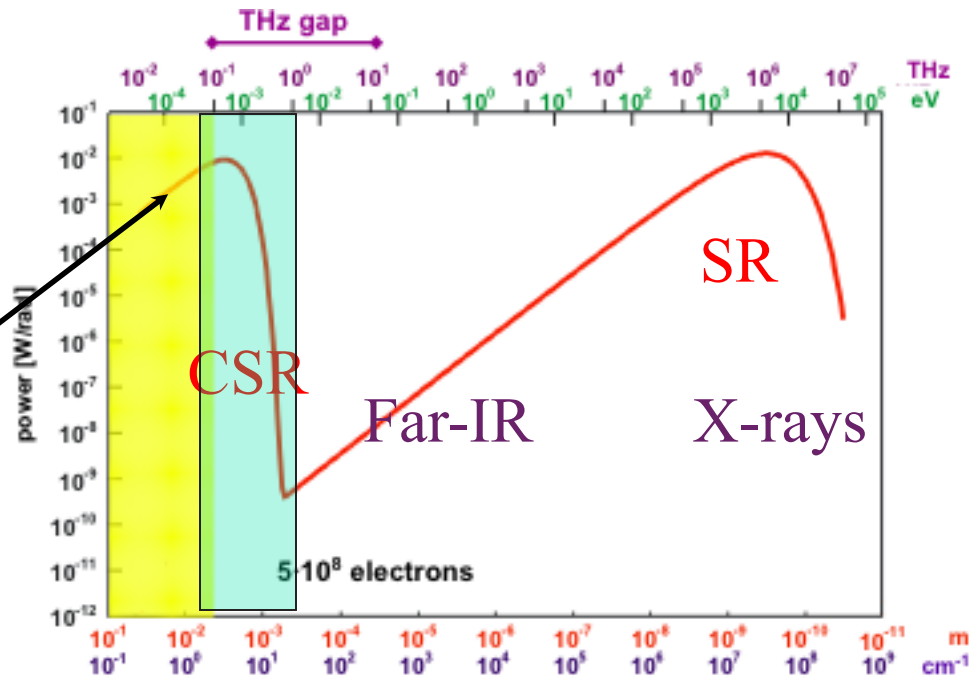

Production of Coherent Synchrotron Radiation

Two main methods in a Synchrotron Machine

Low-α mode

Needed to change the magnetic optics:
Only dedicated runs

Low-e beam energy

Injected the machine at low-E:
Reducing life-time and stability

Momentum compaction factor α : **$\Delta p/p=\alpha=\sigma/L$**
Where σ is the bunch length and L is the length of the ideal trajectory inside the machine

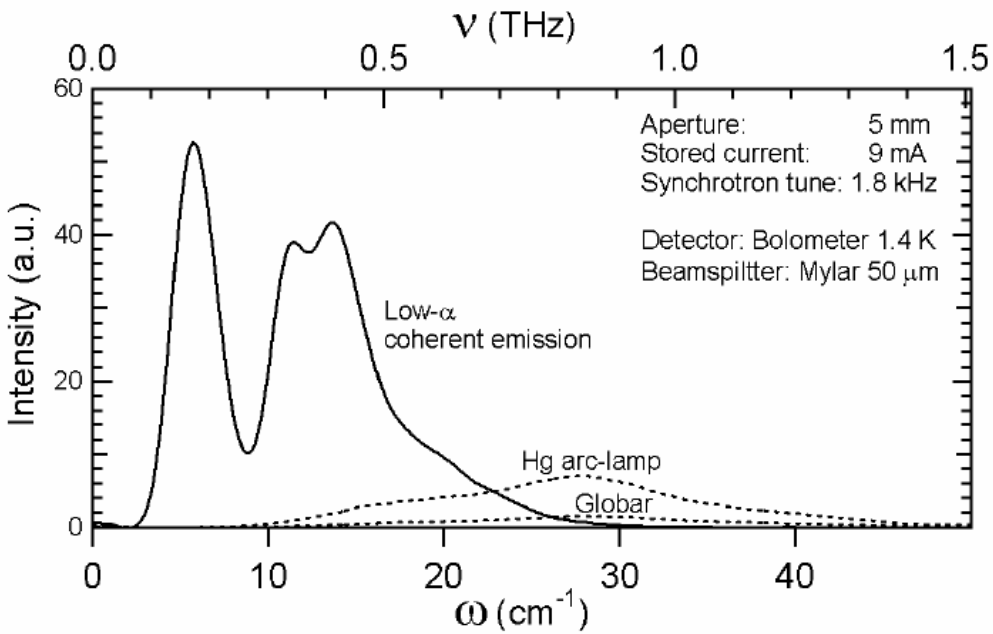

IRIS@Bessy-II: U. Schade et al, PRL 2003

$\sigma \approx E^{2/3}$

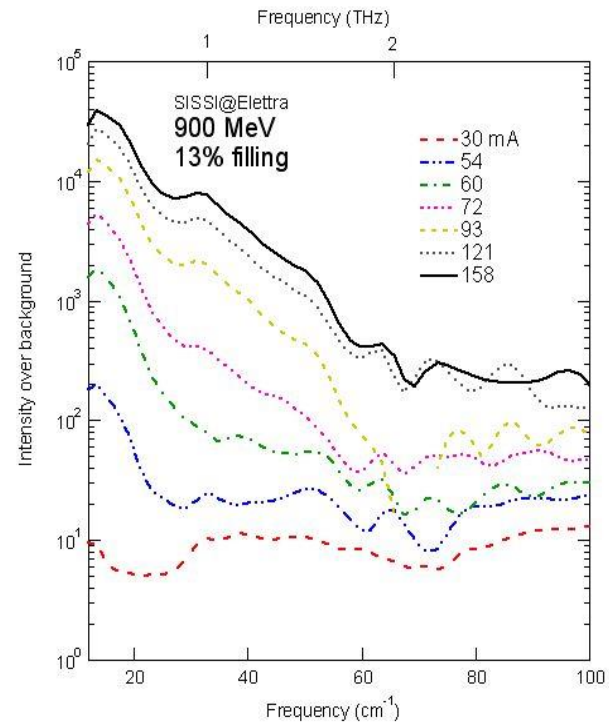

SISSI@Elettra: E. Karanzoulis, A. Perucchi and S.L.,2007

Instrumentation I
Measuring a source power spectrum: Michelson Interferometer

A Michelson Interferometer is based on the interference effect among the two *em* waves at the beam-splitter site

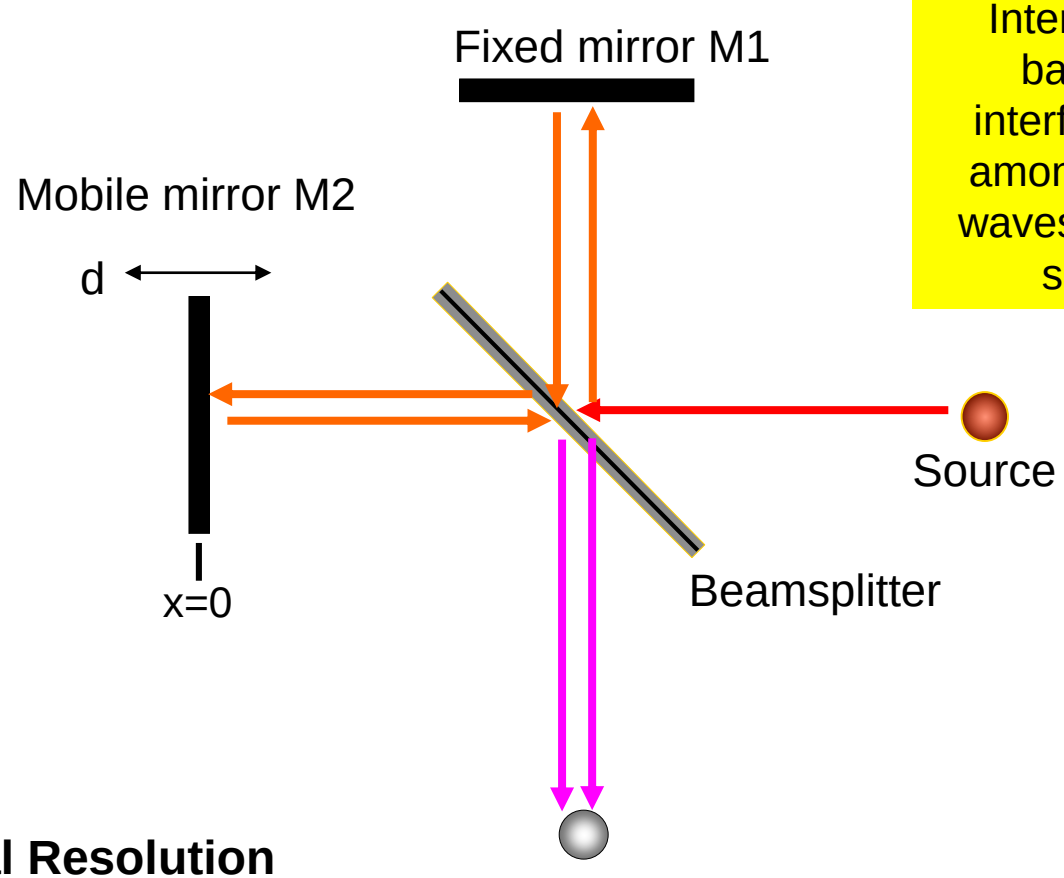

Spectral Resolution

$\Delta\nu \sim 1/d$ (cm^{-1}) ~ 0.001 cm^{-1} ~ 1μeV

Detector → Measure of the figure of interference

Interferogram

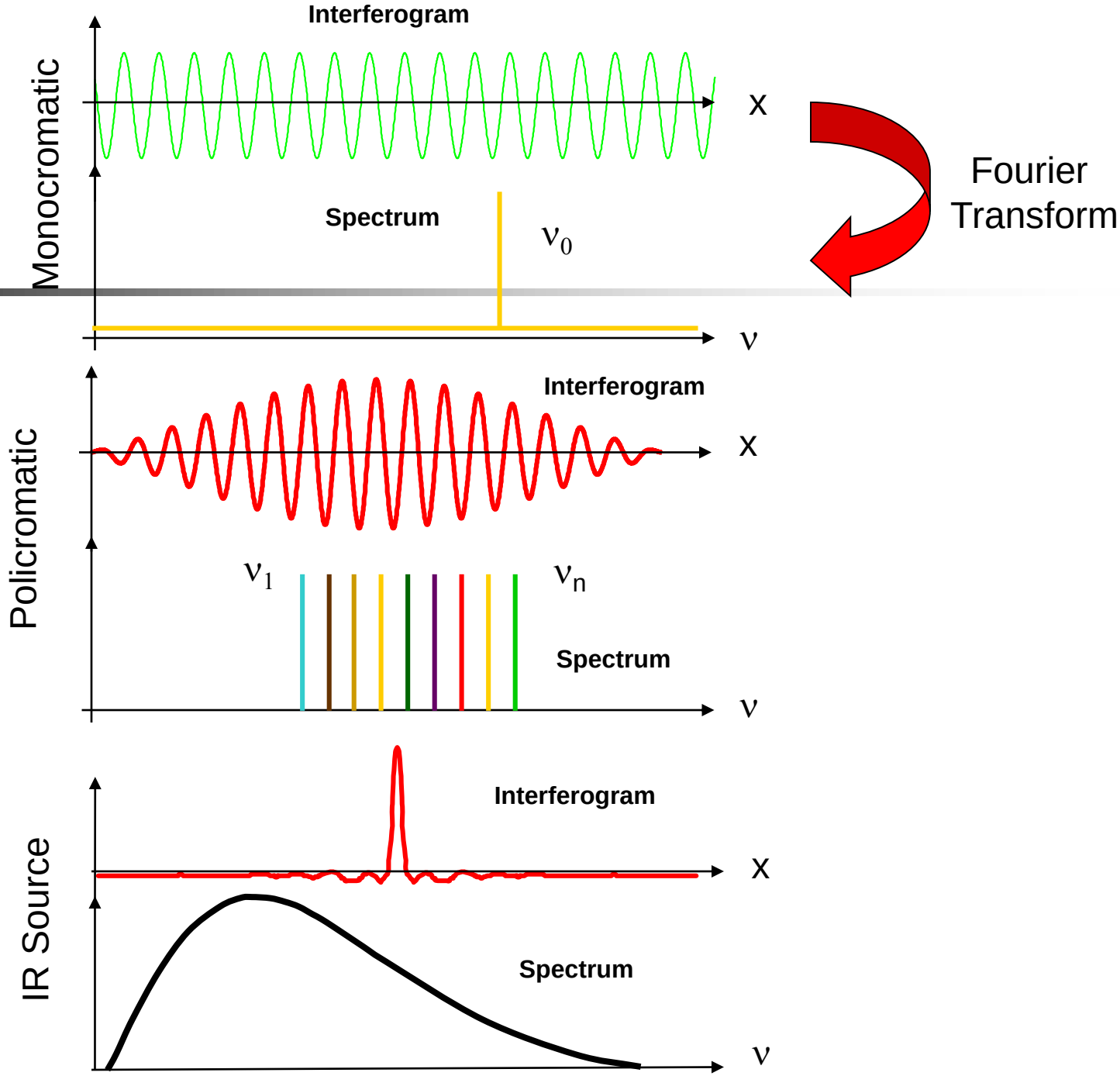
Interferogram
Monocromatic
x
Spectrum
ν_0
Fourier Transform
ν
Interferogram
Policromatic
x
ν_1
ν_n
Spectrum
ν
Interferogram
IR Source
x
Spectrum
ν

Instrumentation II
Infrared Microscopy

Infrared Microscope---->Beam Condenser

Visualize and measure small and/or no-homogenous sample (size<100 μm) with a high spatial resolution

Bruker-Hyperion

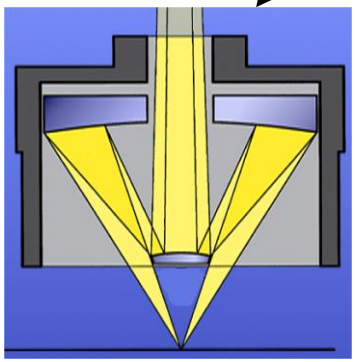

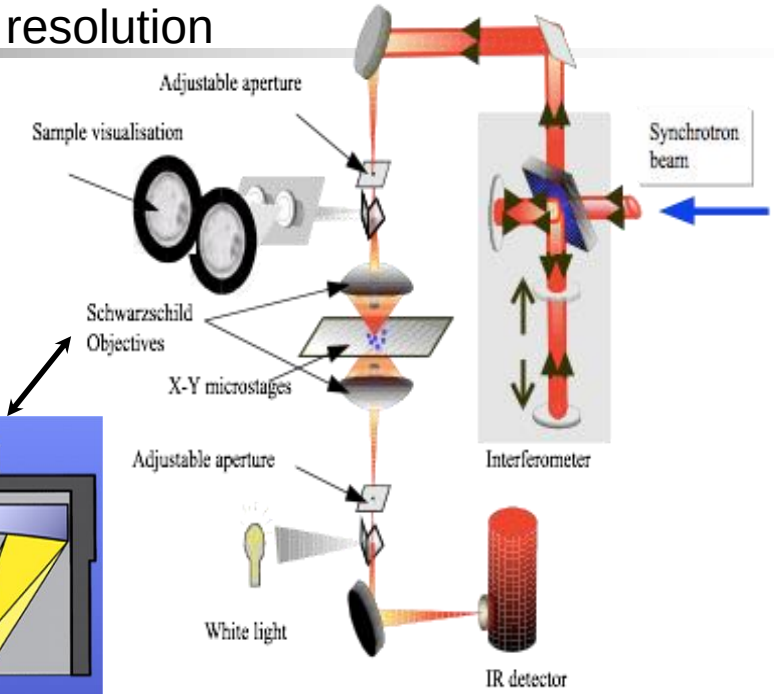

In the IR spatial Resolution is determined by diffraction

$$\delta = 0.61\frac{\lambda}{NA} \approx \lambda$$

For example with a 36x objective with NA=0.5, one obtains:

at λ = 10 μm (1000 cm^{-1}):12 μm

at λ = 2.5 μm (4000 cm^{-1}):3 μm

Experimental Techniques

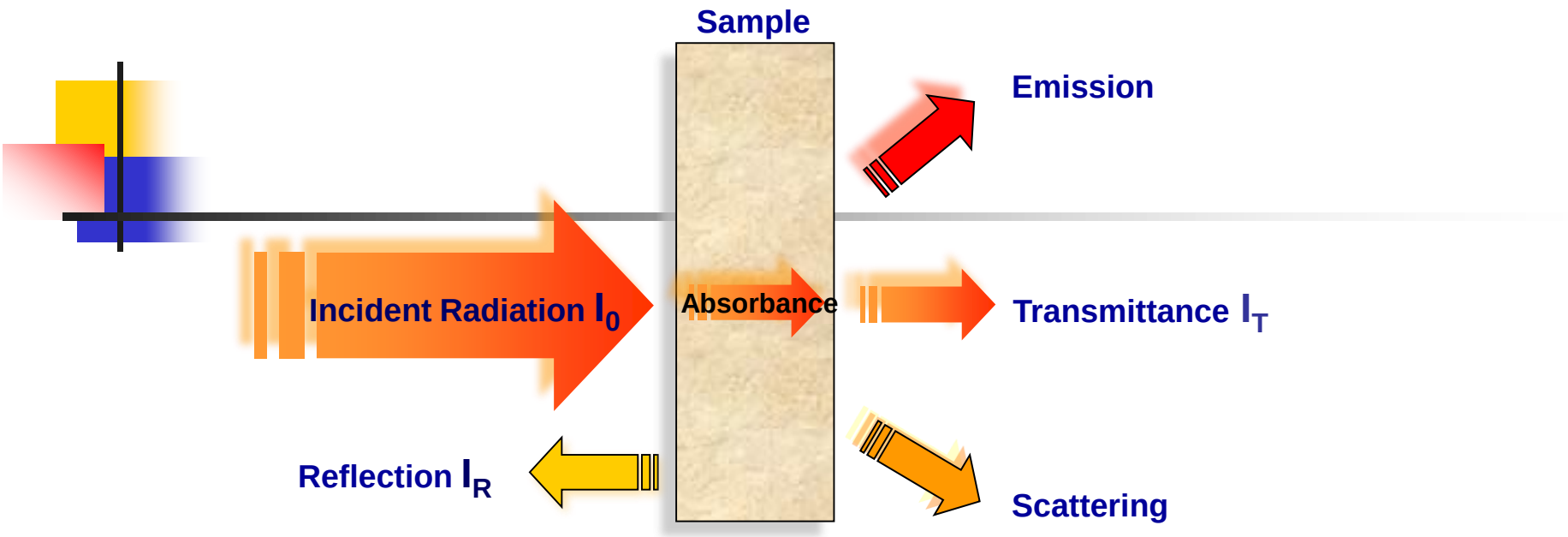

Reflectivity, Transmittance, and Absorption R+T+A=1

$$R(\omega) = \frac{I_R(\omega)}{I_0(\omega)}$$

$$R(\omega) = \frac{(n-1)^2 + k^2}{(n+1)^2 + k^2}$$

Via **Kramers-Kronig** Transformation real and immaginary part of the optical response functions (n, ε, σ) can be obtained

$$\tilde{n} = \sqrt{\tilde{\varepsilon}}$$

$$\varepsilon_1 = n^2 - k^2 = \varepsilon_\infty - \frac{4\pi}{\omega}\sigma_2$$

$$\varepsilon_2 = 2nk = \frac{4\pi}{\omega}\sigma_1$$

Reflectivity experiments

Interferometer

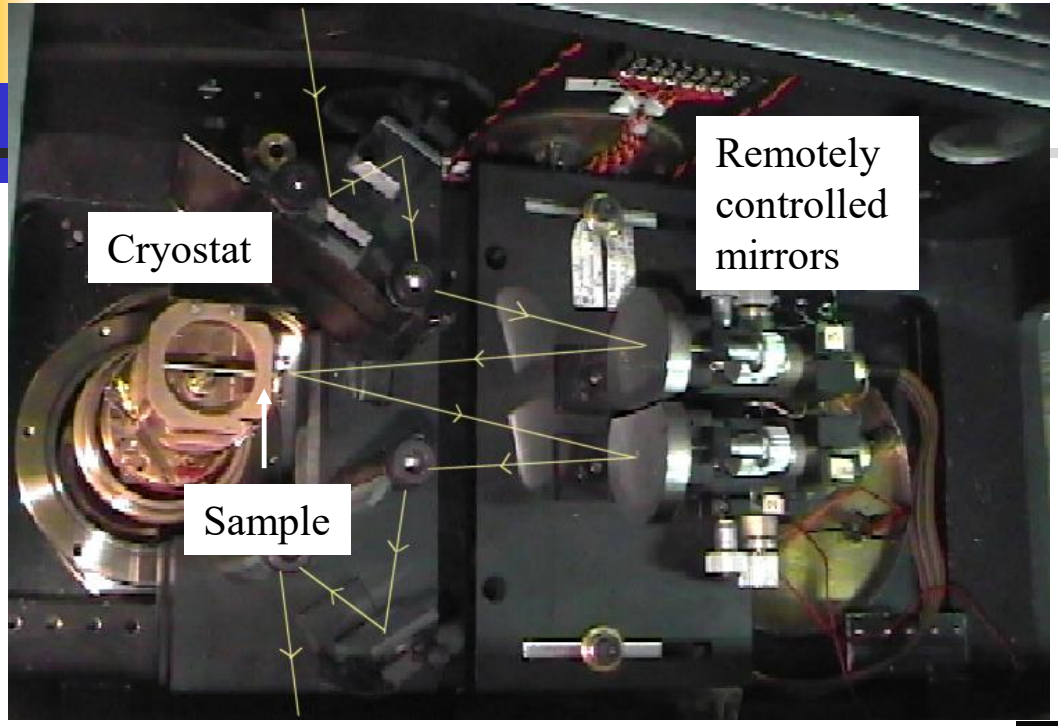

Detector

Reference:
gold evaporated *in situ*
Reflectivity:
$R = I_R^{crys} / I_R^{gold}$
$\Downarrow$
Kramers-Kronig transf.
$\Downarrow$
optical conductivity
$\sigma(\omega)$

Single crystals may be very small:

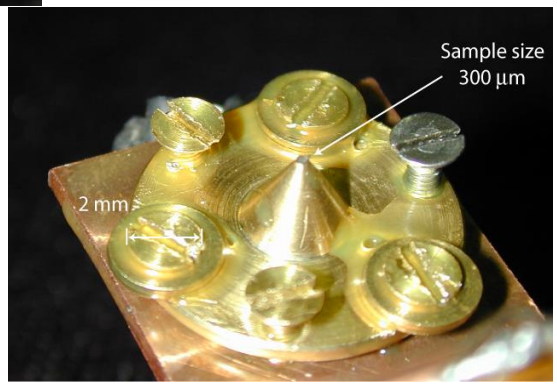

Solid-State Applications I
Superconductivity

(FLUX GAIN)

Superconductivity today

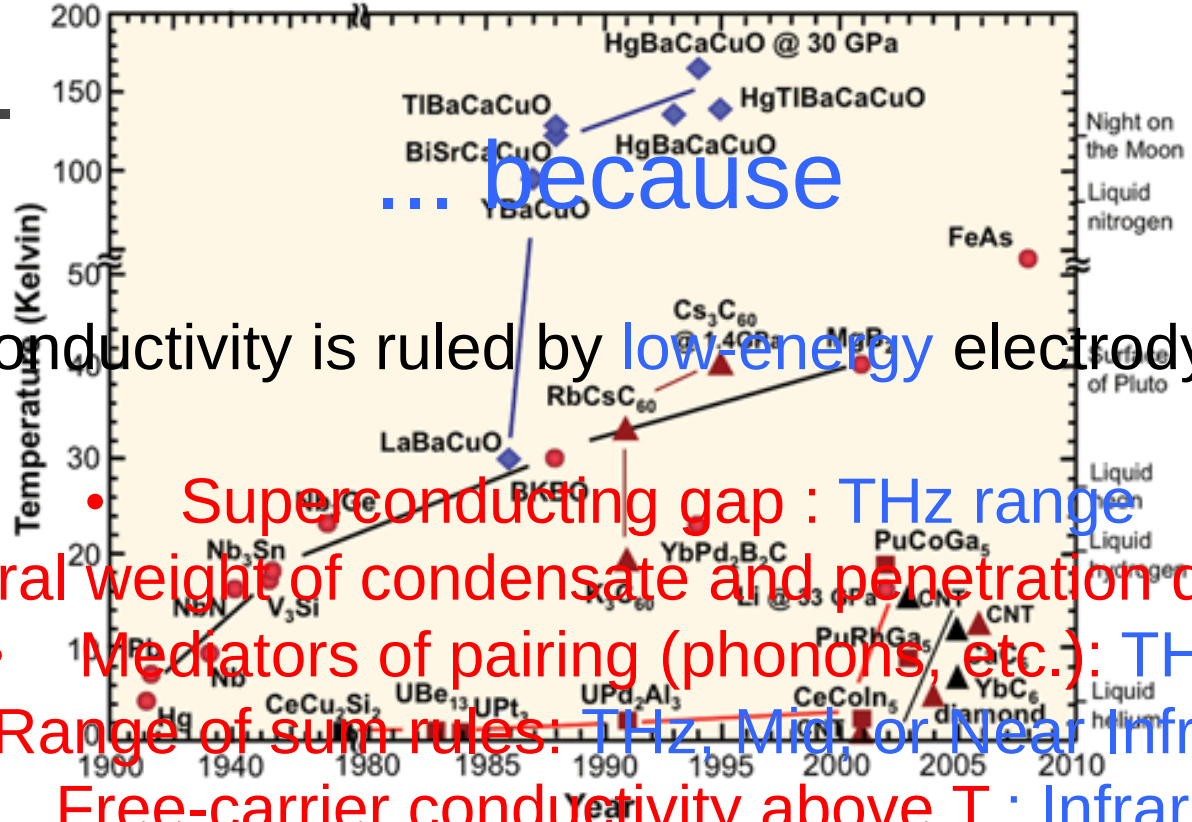

... because

Superconductivity is ruled by low energy electrodynamics:

- Superconducting gap : THz range
- Spectral weight of condensate and penetration depth: THz
- Mediators of pairing (phonons, etc.): THz
- Range of sum rules: THz, Mid or Near Infrared
- Free-carrier conductivity above T_c: Infrared

Infrared and THz spectroscopy plays a fundamental role

Basic optics of Superconductors

Minimum excitation energy:
Cooper-pair breaking 2Δ

Superconducting gap observed if:
- sample in the dirty-limit ($2\Delta < \Gamma$)
- Cooper pairs in s-wave symmetry

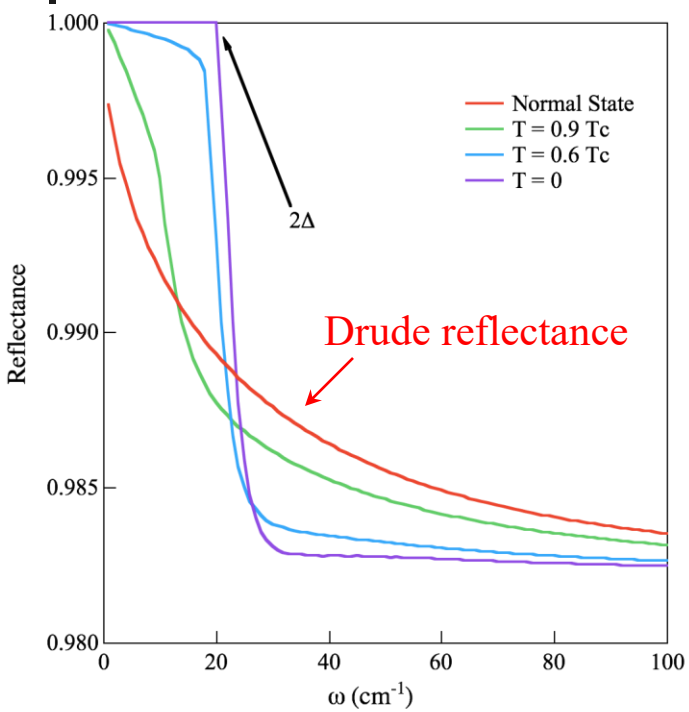

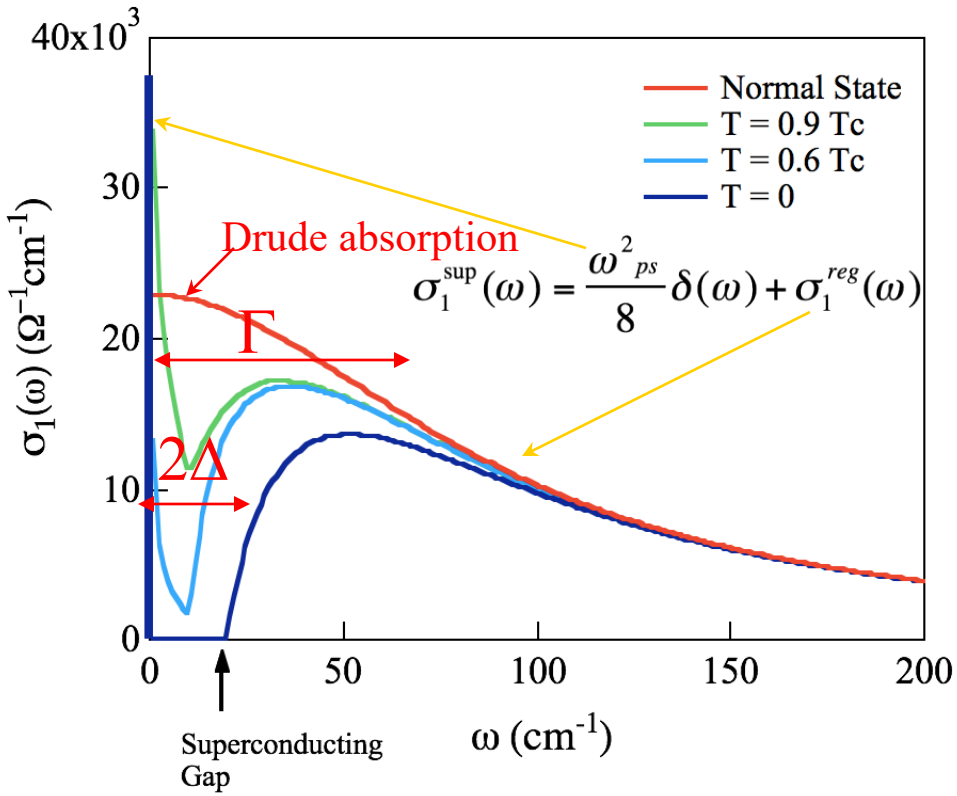

$$\int [\sigma_1(\omega, T>Tc) - \sigma_1(\omega, T<Tc)]\, d\omega = \omega^2_{ps}/8 = n_s e^2/m^* \dashrightarrow \lambda = c/\omega_{ps}$$

Ferrel-Glover-Tinkham Rule

THz Reflectivity of Superconducting Diamond

$\omega \leq \Gamma(T)$: $R_n(\omega) = 1 - [8\omega\Gamma(T)/\omega_p^2]^{1/2}$ $\omega \leq 2\Delta(T)$: $R_s(\omega) = 1$

Peak at 2Δ in Rs/Rn

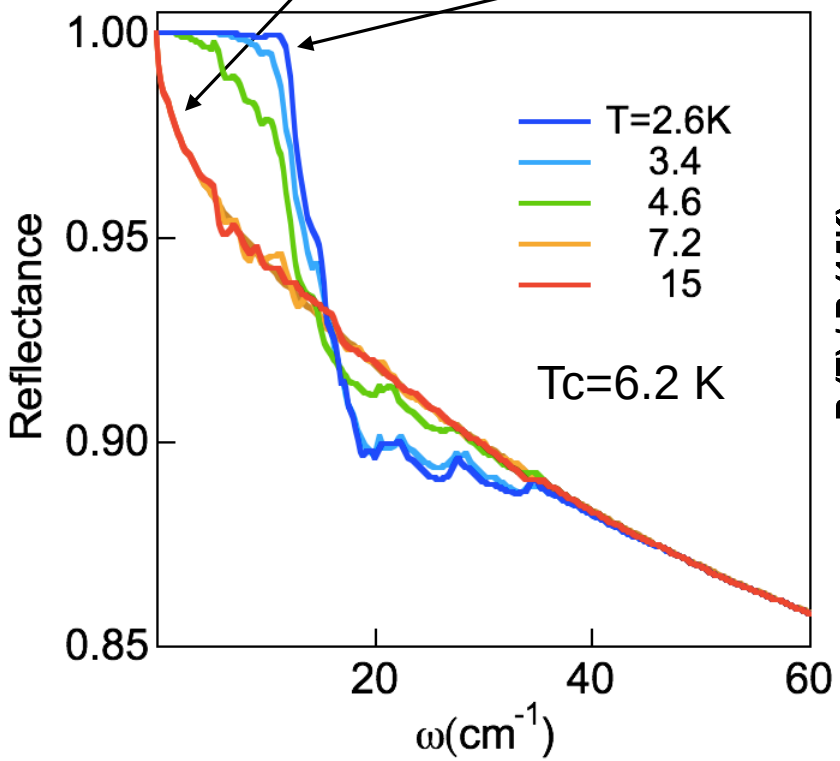

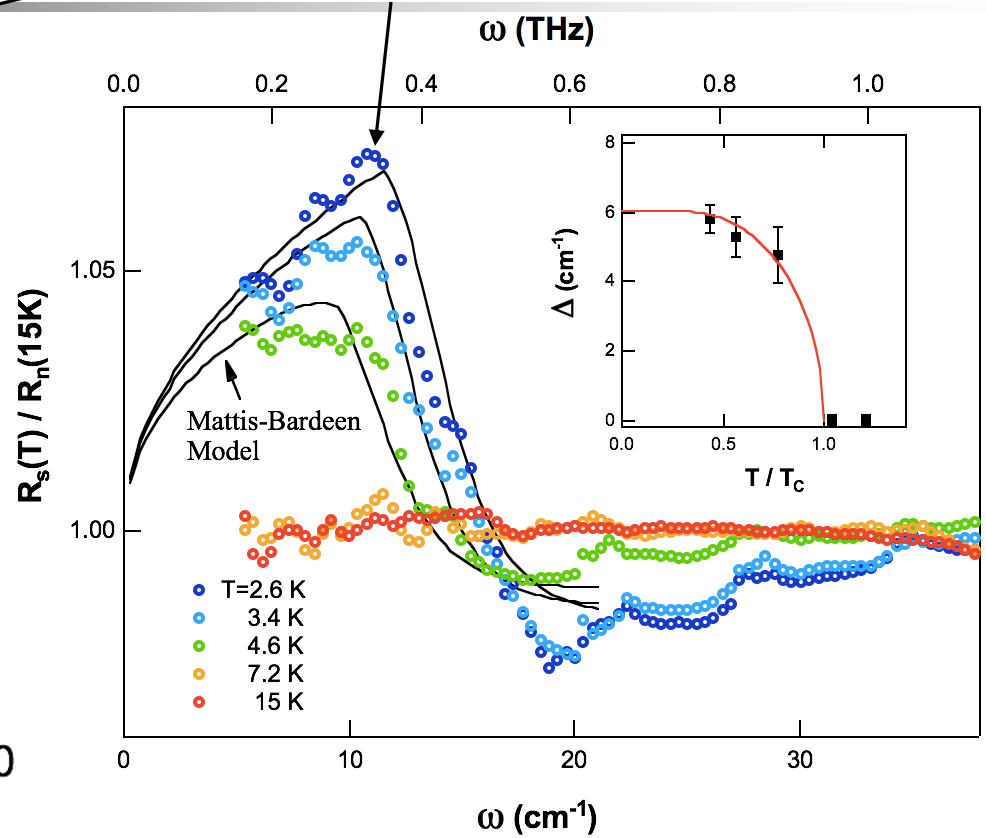

s-wave Dirty-Limit Regime; $2\Delta(2.6\ K)=12\pm1\ cm^{-1}$ ➡ $2\Delta/k_BT_C=3.2 \pm 0.5$

M. Ortolani, S. L. et al, PRL 2006

Solid-State Applications II
Metal-to-Insulator Transition (MIT)

(BRILLIANCE GAIN)

Insulator to Metal Transitions

Many materials are insulating although band theory suggests a metallic ground state: V_2O_3, VO_2, NiO, $NiSe_2$, La_2CuO_4, Cs_3C_{60}

→Strong Electronic Correlations→Hubbard Model

$$H = -t \sum_{<ij>\sigma} (c^{+}_{i\sigma} c_{j\sigma} + h.c.) + U \sum_{i} n_{i\uparrow} n_{i\downarrow}$$

U Coulomb repulsion

t Bandwidth

U prevents double on-site occupancy → a gap in the spectra of excitations is induced

How to transform an Insulator in a Metal

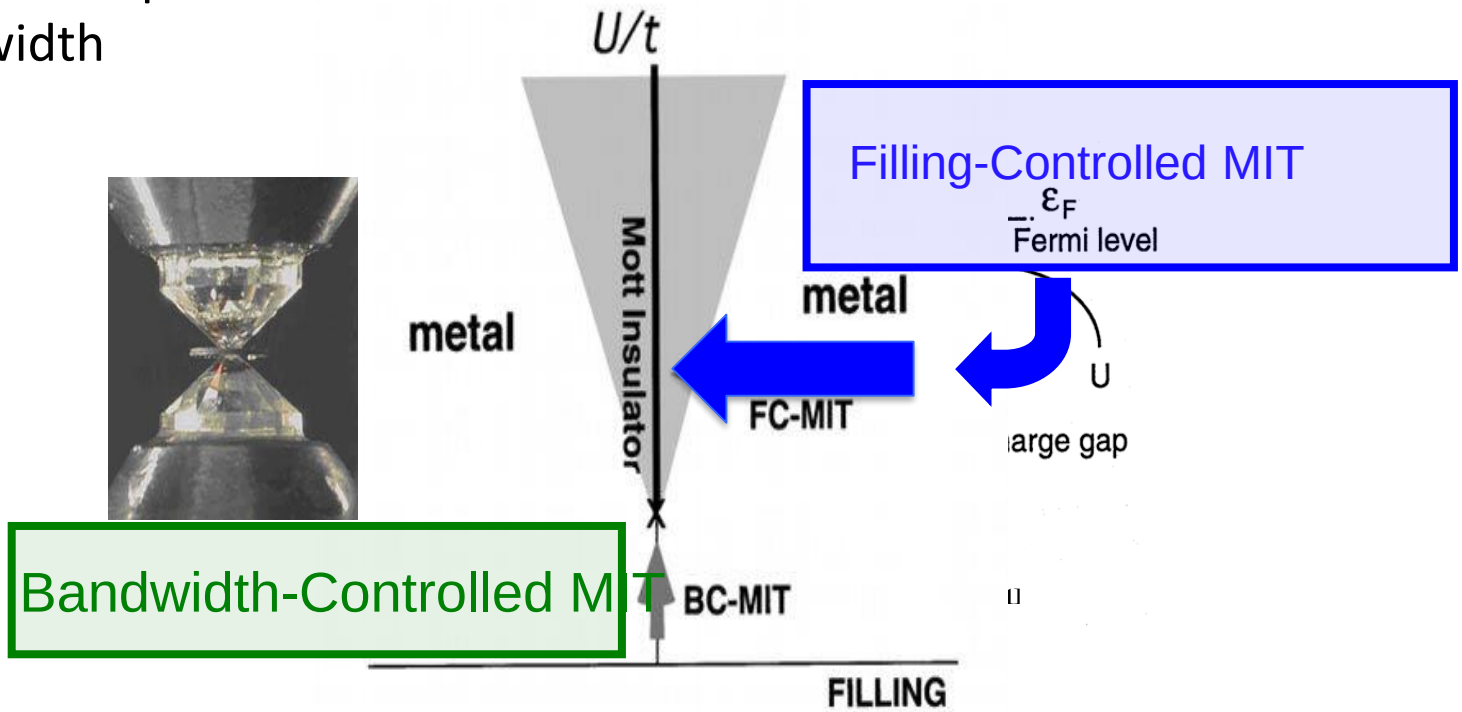

IRSR Microscopy at high pressures

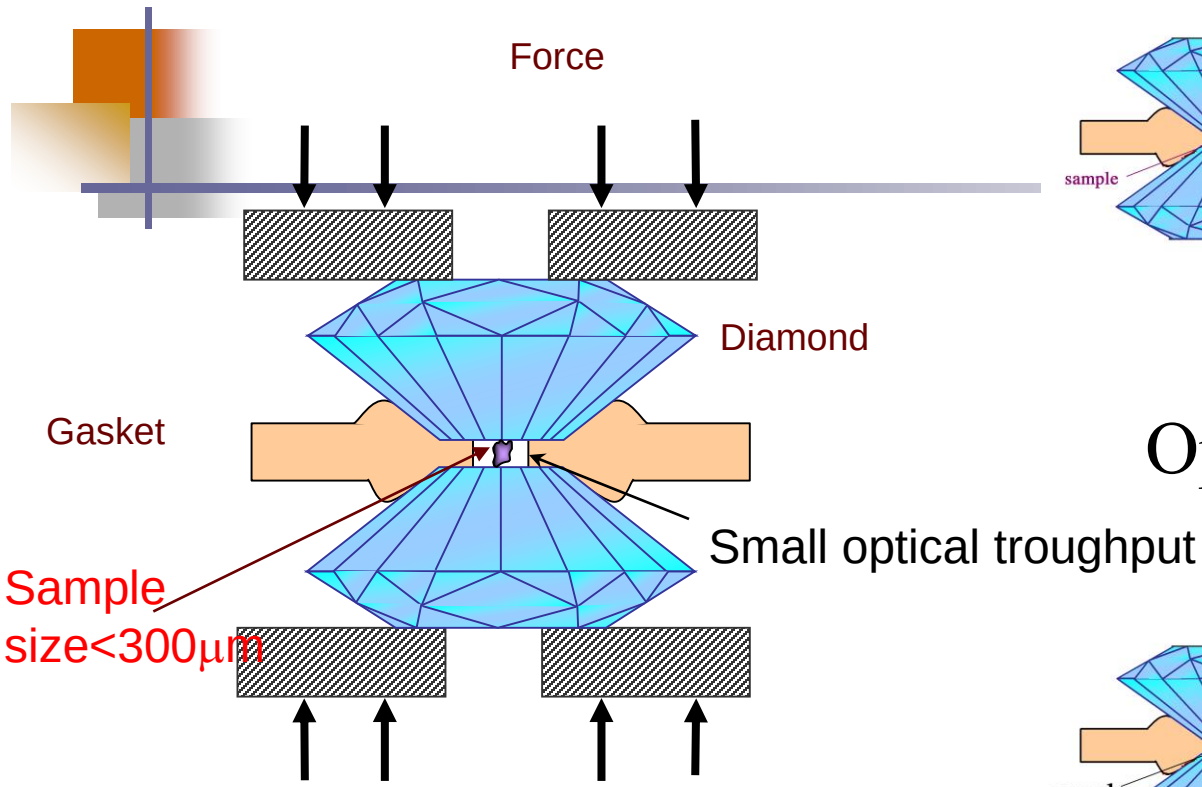

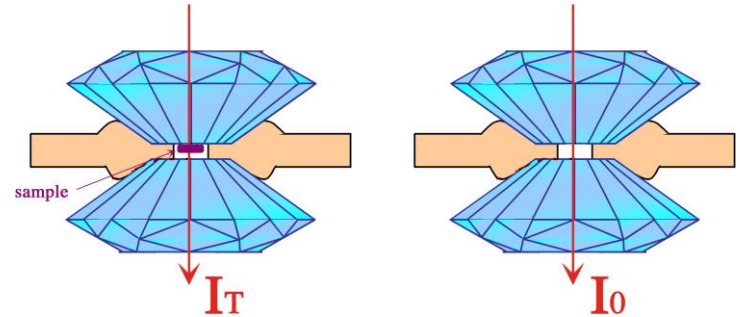

$$T = I_T / I_0$$

$$\text{Op.D.} = -\ln(T) = \alpha d$$

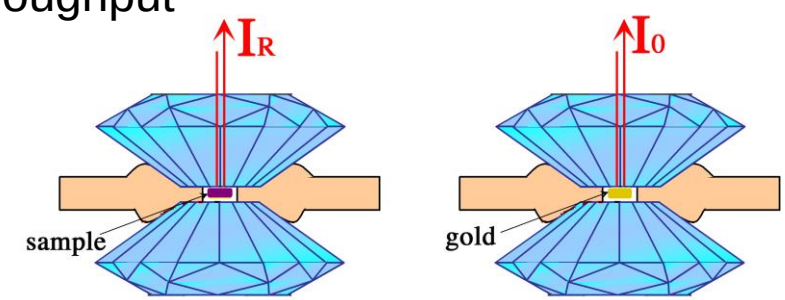

$$R_{diam/sam} = I_R / I_0$$

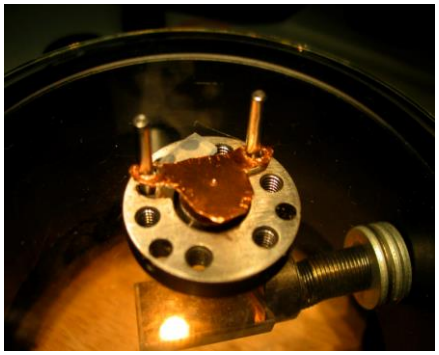

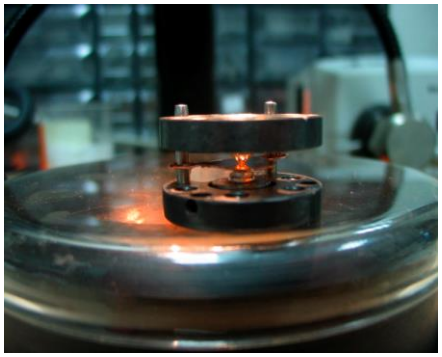

THz Reflectivity of Superconducting H3S

P=155 GPa

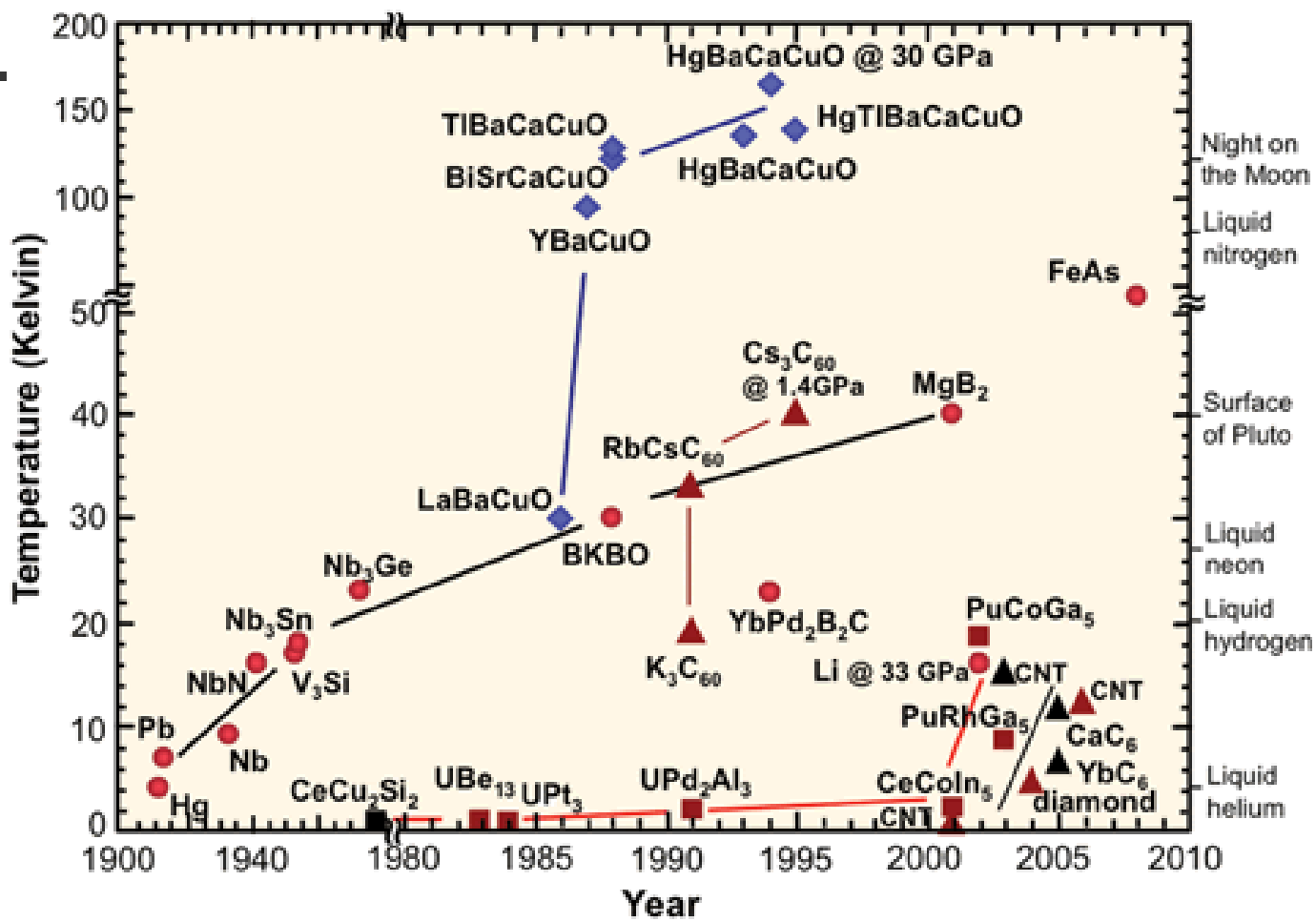

H3S
150 Gpa
Tc=200 K

F. Capitani et al., Nature Physics 2017

Generalities on Vanadium dioxides VO_2

Metal

T>340 K

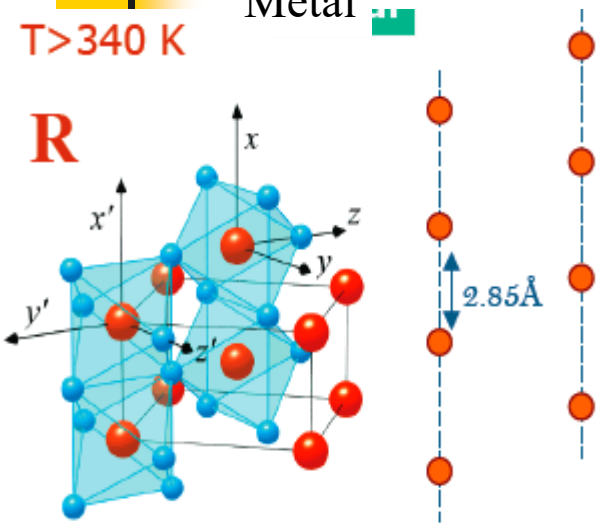

T-dependent MIT at T_{MIT}= 340 K
Concomitant lattice modification from an low-T monoclinic (M1) phase to a high-T rutile (R) phase.
<u>Both phases are non-magnetic</u>

Insulator
dimers
along c

T<340 K

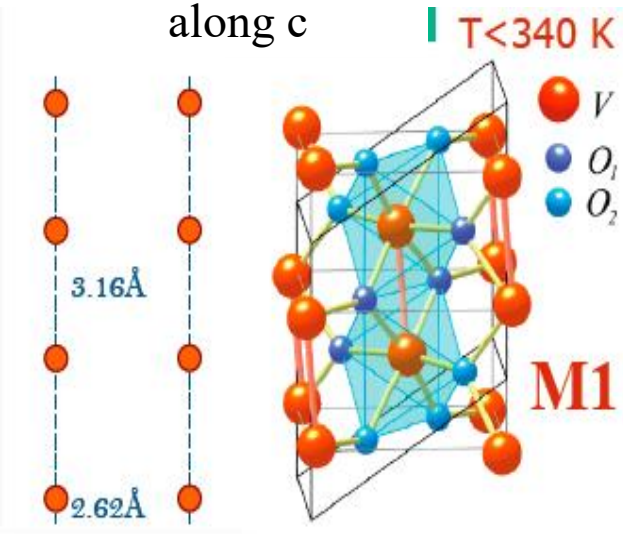

Strong Interplay between electron-lattice and electron-electron interactions

Driving MIT mechanism Hubbard or Peierls?

High Pressure may disentangle the two mechanisms

P-dependent infrared measurements on VO_2

Simultaneous measurements of reflectance and transmittance at 300 K in the M1 monoclinic insulating phase on a thin VO_2 sample

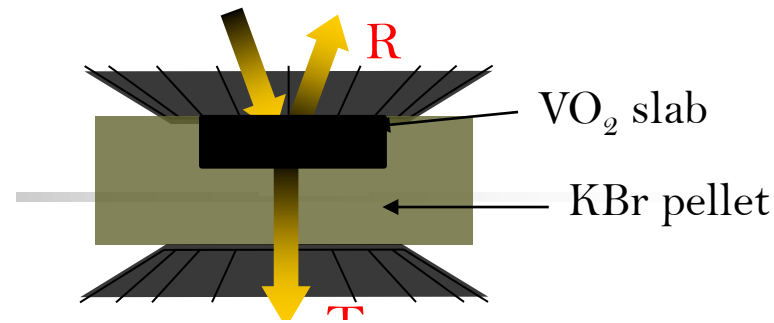

Pressure induces a metallization process in a new monoclinic structure Mx

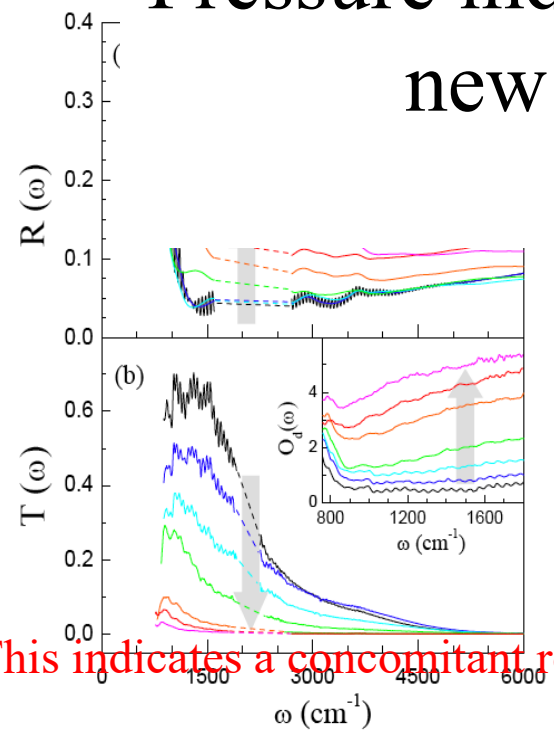

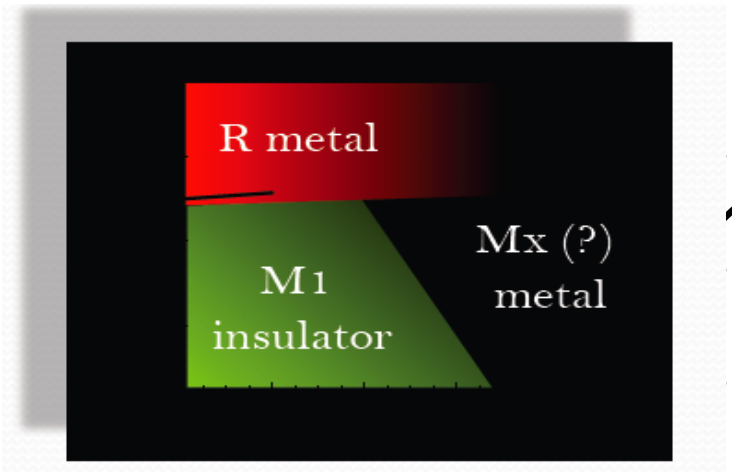

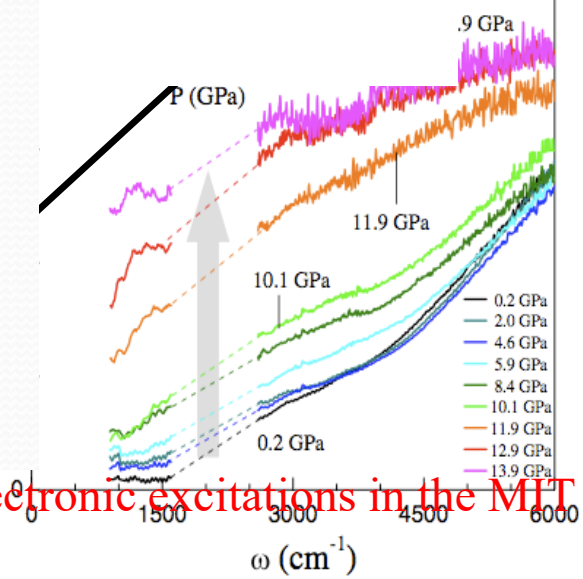

This indicates a concomitant role of lattice (GPa) phonons and electronic excitations in the MIT

E. Arcangeletti et al, Phys. Rev. Lett. 98, 196406 (2007)

Pressure Induced Polimerization of Polyacetylene in Zeolite

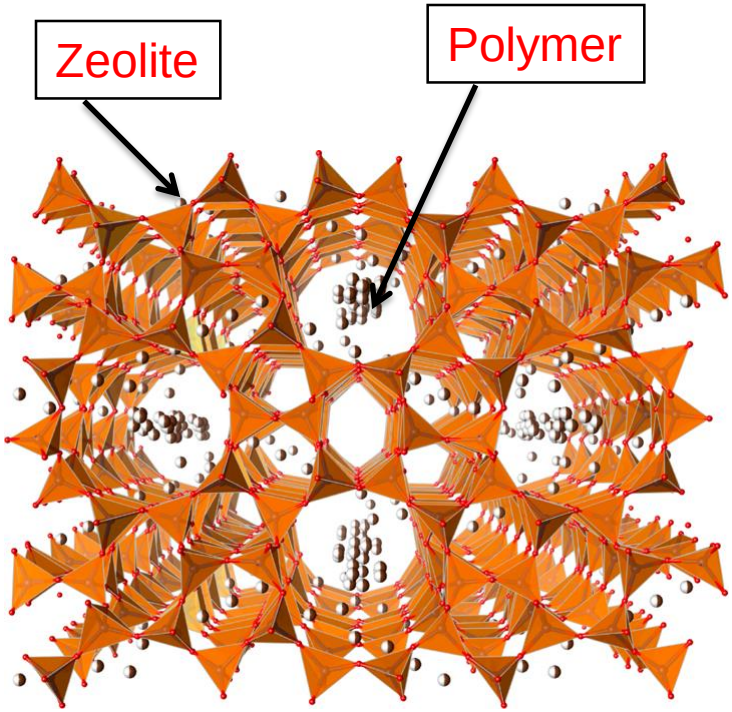

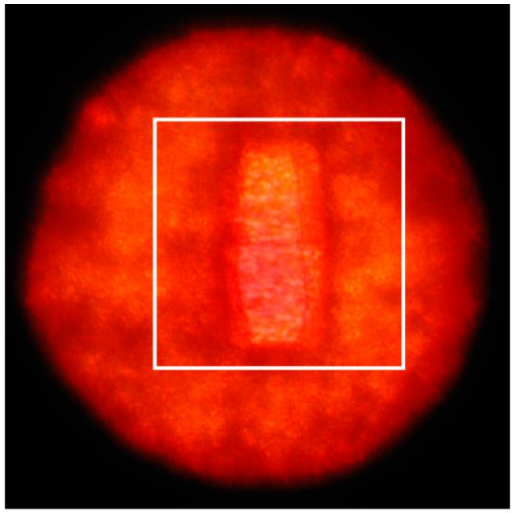

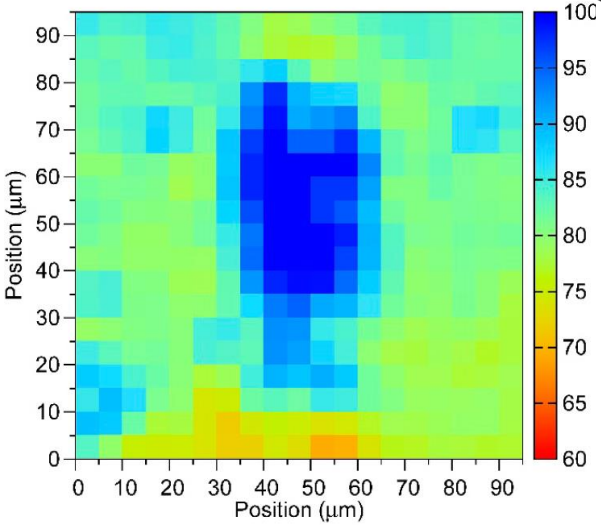

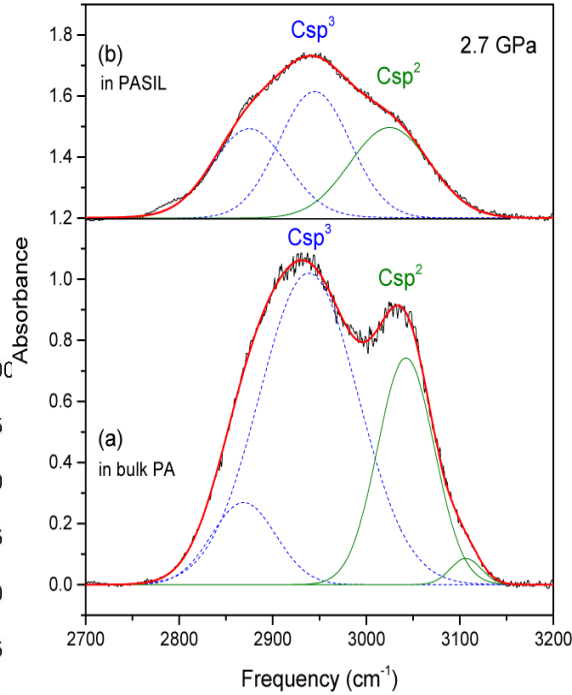

D. Scelta et al, Chemistry of Mat. 2014

Medical and Biological Application of IR Microscopy

How look the IR spectrum of a cell?

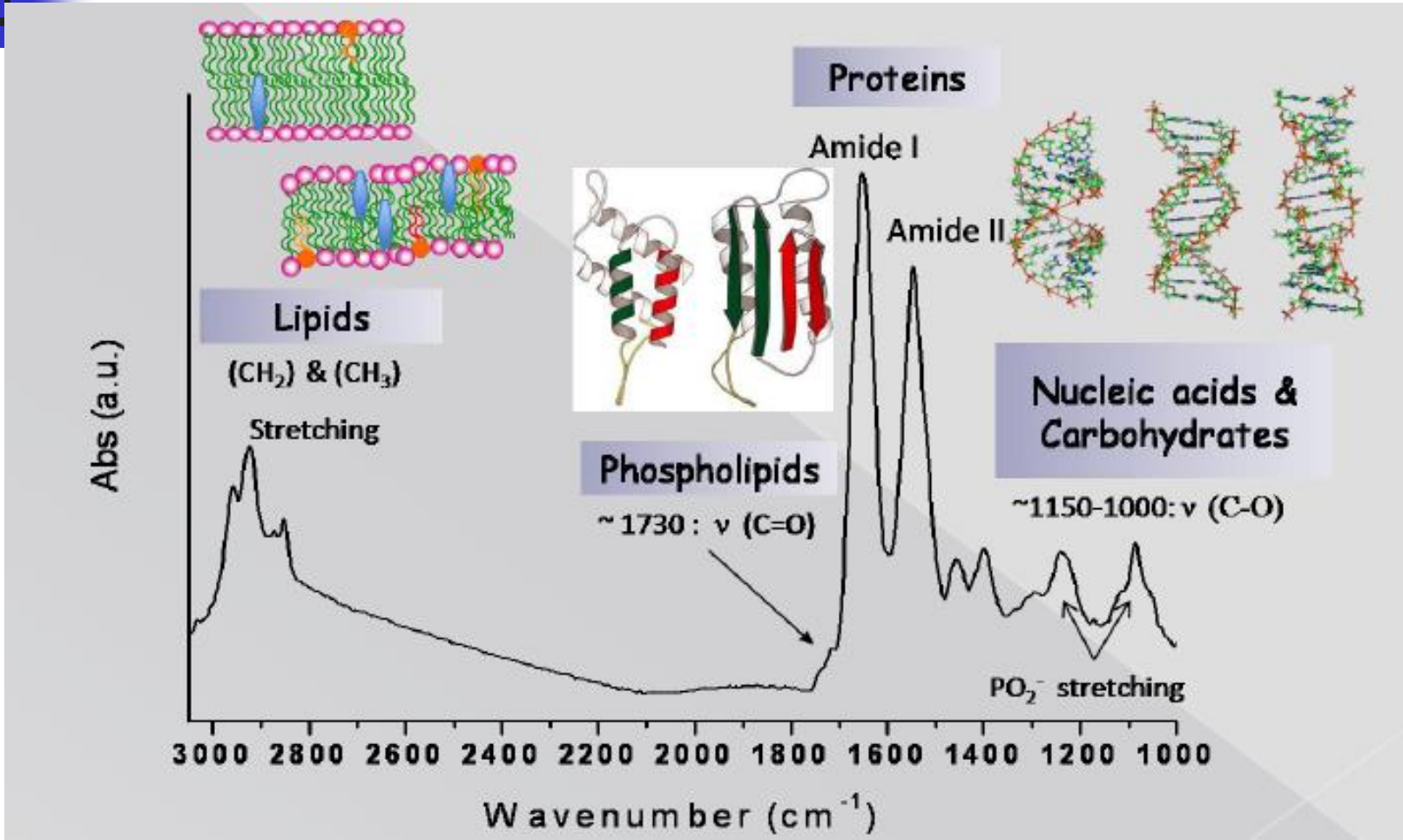

Vibration Frequencies correspond to finger-print for the molecule

Infrared Group frequency region

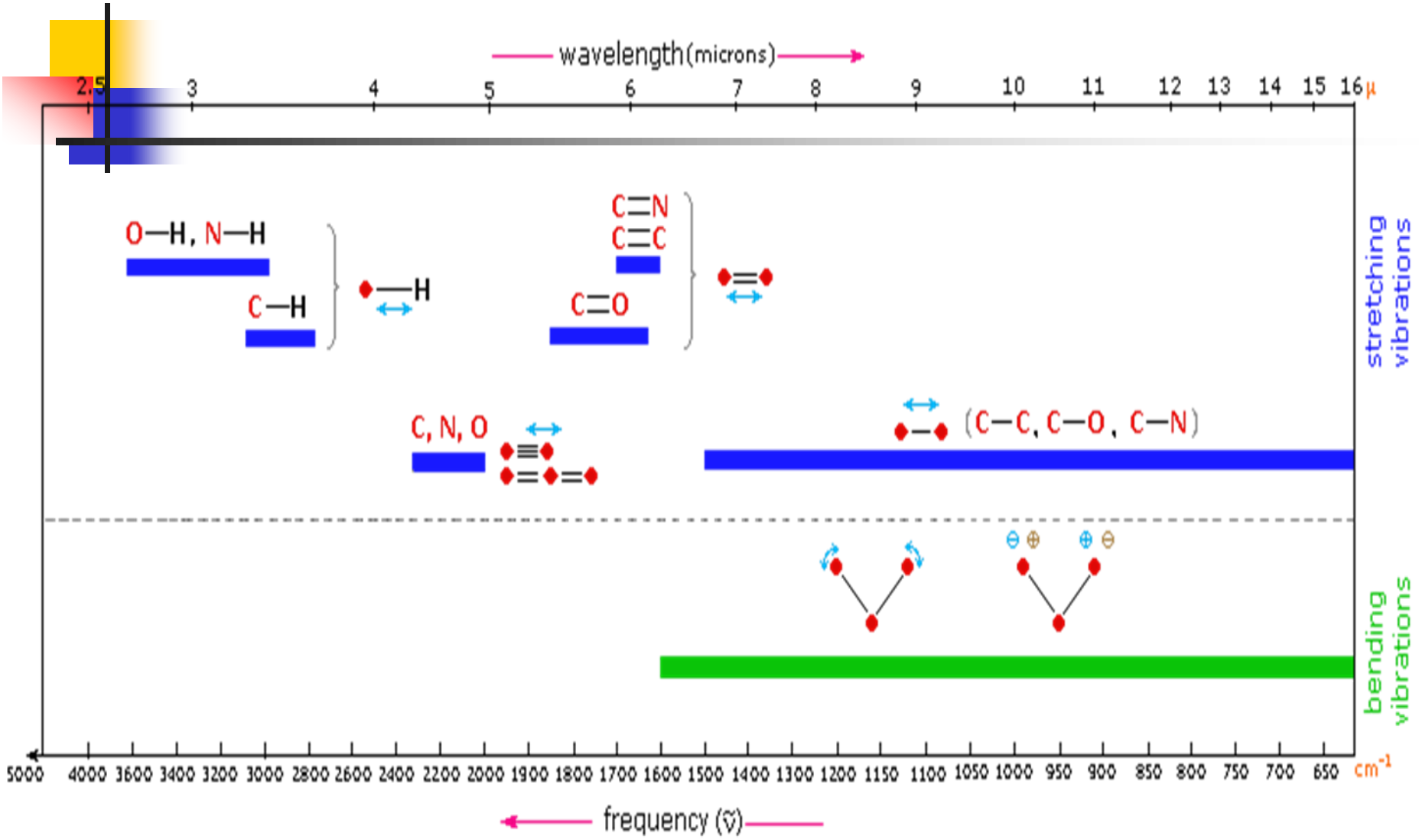

IRSR spectrum of a single cell during mitosis

The cell physiology is not altered under IRSR illumination

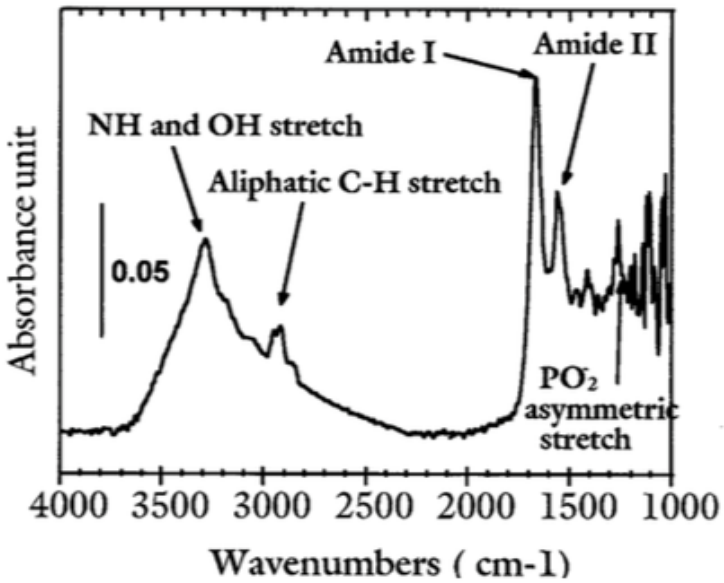

FIG. 1. Infrared spectrum of a mouse UN2 hybridoma B living cell, recorded with an aperture of 3×3 μm^2. The instrumental resolution was set at 4 cm^{-1}, and the spectrum displayed is the result of 128 co-added scans (the total recording time is 55 sec).

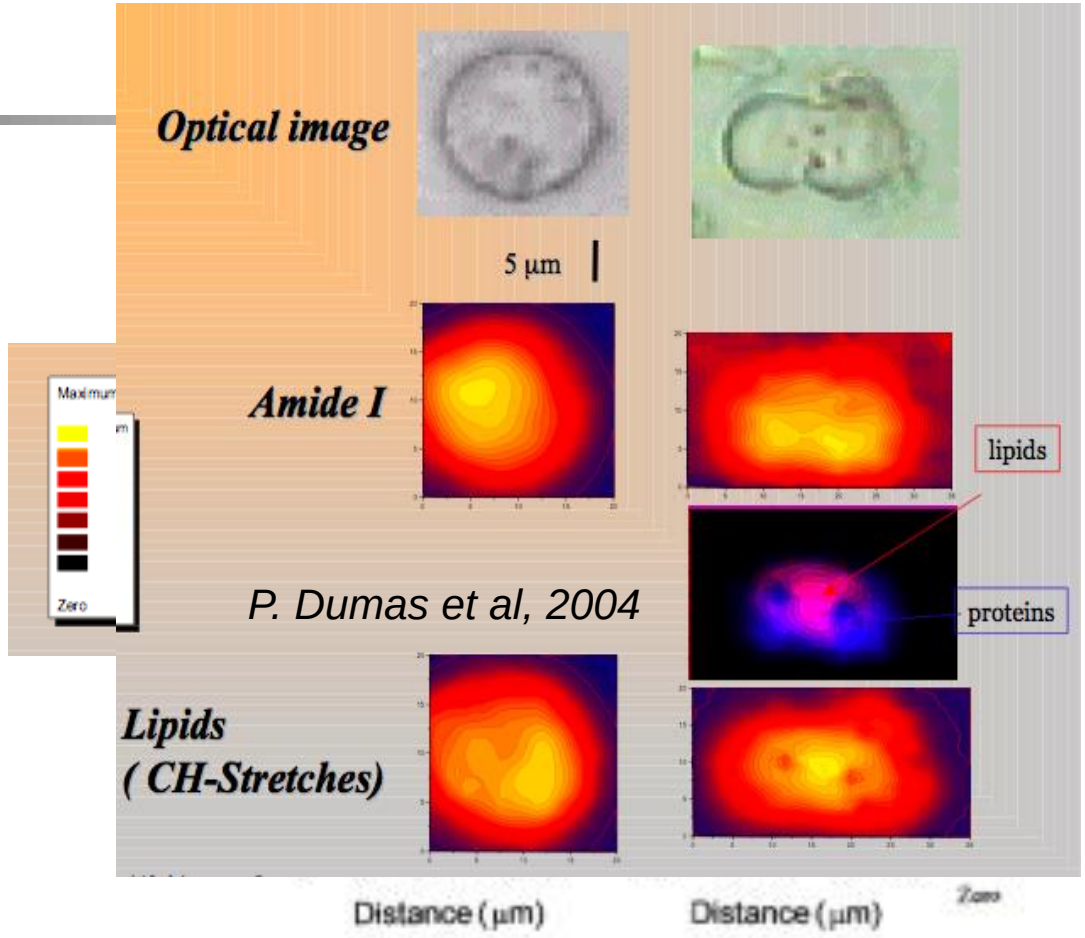

P. Dumas et al, 2004

Spatial distribution of proteins and lipids in a cell

Spatial distribution of proteins and lipids during the cell mitosis

P. Dumas et al, 2004

Studying hair by IRSR microscopy

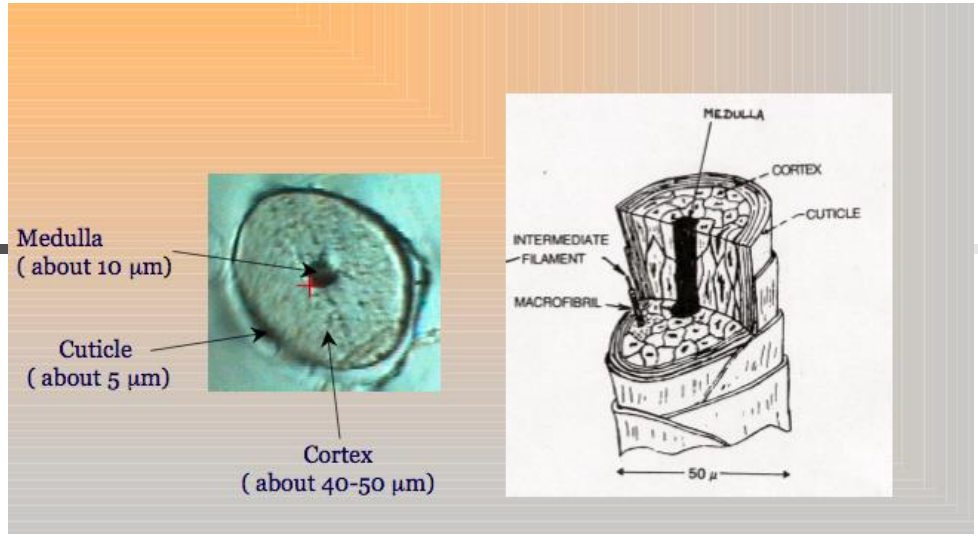

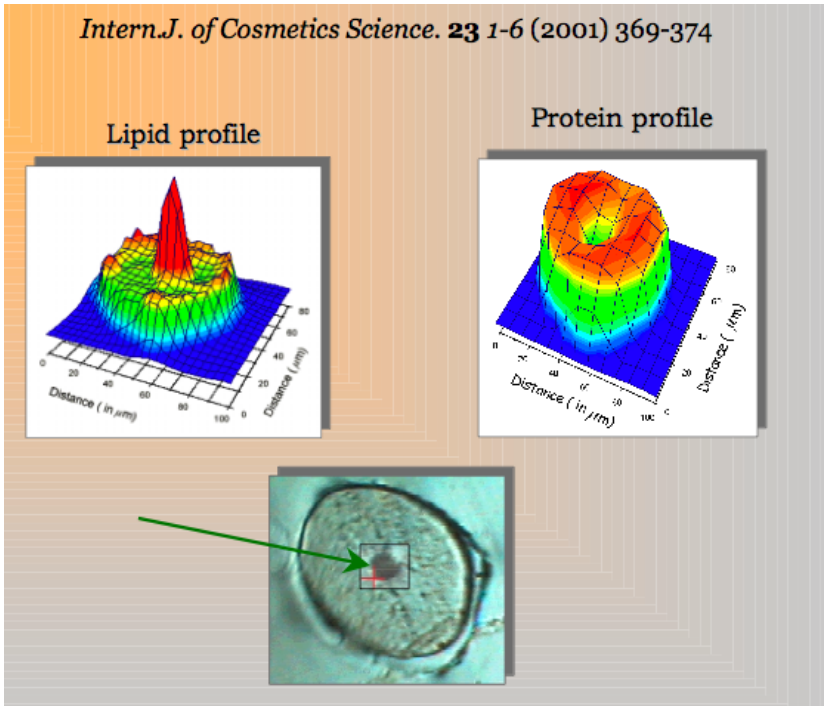

P. Dumas et al, 2004

Geological Applications: liquid inclusion in minerals

Brilliance gain

Liquid Inclusion in quarzite

Mapping with 3μm x 3μm (diffraction limited)

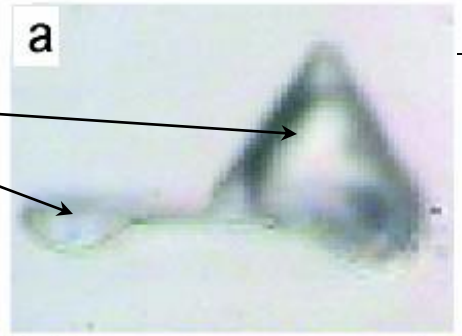

3μm

Optical Image

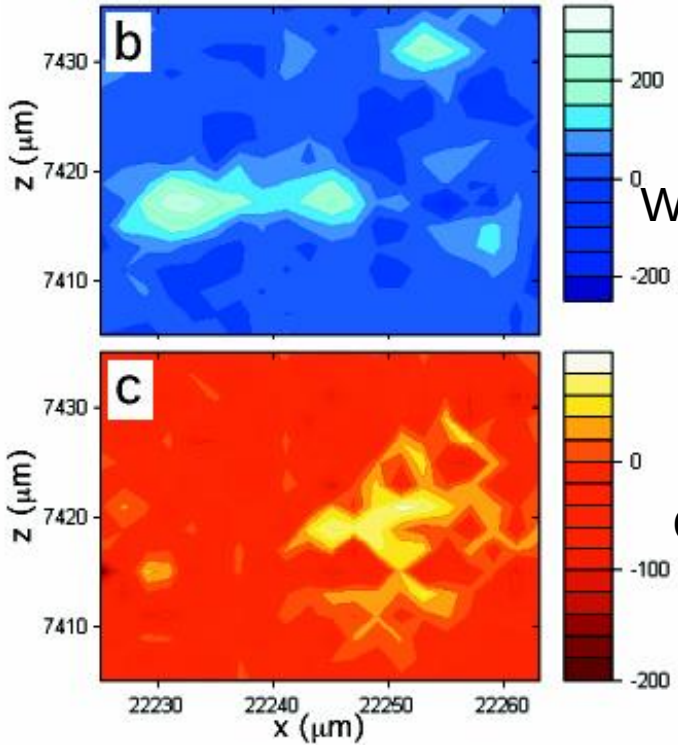

Water Distribution

CO_2 Distribution

Infrared Spectra

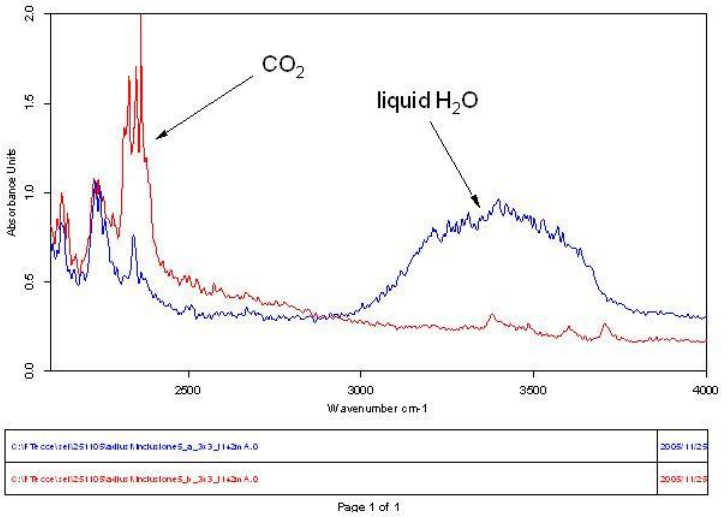

A. Perucchi, S.L. et al, 2006

Interstellar micron size dust analysis

comparison SRS-Black body:

3 micron Particles from asteroid "Orgueil"

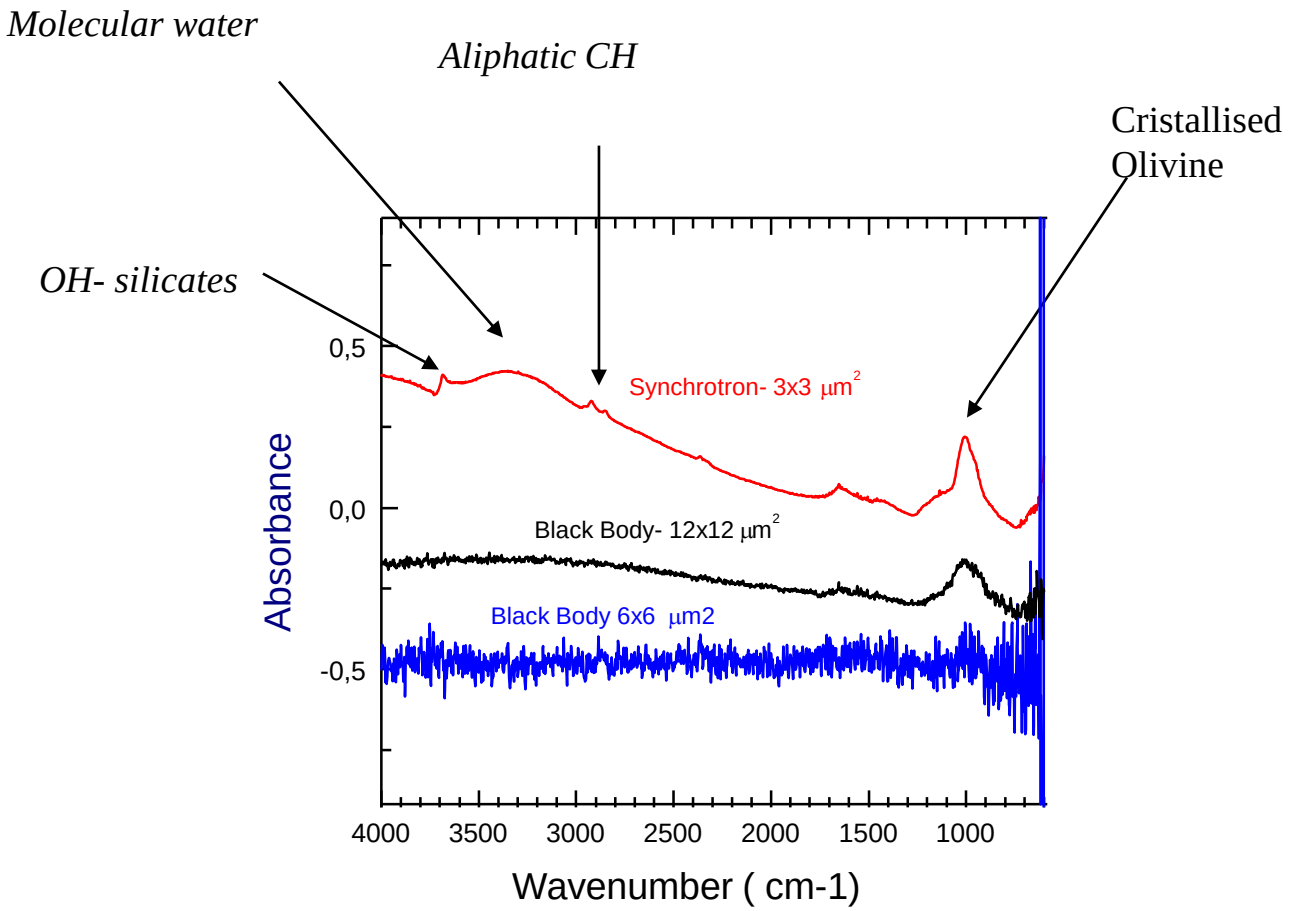

Particles collected from the MIR shuttle

Recent Developments

1. THz IV generation sources: Non linear and time-resolved spectroscopy;

2. Beating the diffraction limit→IRSR Nanoscopy

Linear *vs.* Non Linear Spectroscopy

Linear Spectroscopy

Low Power Source

Small Perturbation→Sample retains its equilibrium properties

Non linear and Time-Resolved Spectroscopy

High Power/Pulse

Strong Perturbation→out of equilibrium states→manipulation of matter through em fields

Linear versus Non-Linear Optical Response

Actually the linear/non-linear electrodynamics regimes can be estimated through the ratio

$$Q = [\frac{eE}{\omega}] / p_F$$

Electromagnetic Momentum

Fermi Momentum

Linear regime E_{THz} ≈ 10-100 V/cm → Q<<1⟷T=T(ω)⟷σ=σ(ω)

Non linear regime → Q=1

Putting $\omega/2\pi$=1 THz and p_F, Q=1 for E_{THz}≈50 kV/cm→then the optical functions start to be dependent on the applied electric field.

For instance: $T=T(\omega,E_0) \longleftrightarrow \sigma=\sigma(\omega,E_0)$

THz Sources for Non Linear and Pump-Probe Spectroscopy

Figures of merit of a pump source:

1)Energy per pulse ≈1 μJ-10 mJ;
2)Pulse duration→sub-ps scale (more relaxed than in VIS-Near-IR) → an excitation starts to exist after half a cycle (T≈100 fs-10 ps);
3)Rep rate tens of Hz to MHz;
4)Frequency tunability;
5)Associate electric field 100 KV/cm (1 mV/Å) to 100 MV/cm (1V/Å)→Atomic field;
6)Associate magnetic field ≈ 1 T

Coherent Radiation from sub-ps electron bunches

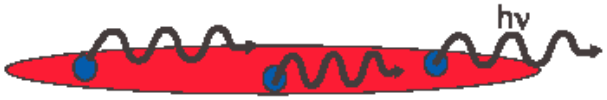

$\sigma_z > \lambda$

Long bunch emits incoherently

$$\frac{d^2 I}{d\omega d\Omega} = \frac{d^2 I_{sp}}{d\omega d\Omega}\left[N + N(N-1)F(\omega)\right]$$

Short bunch emits coherently

$\sigma_z \leq \lambda$

Diffraction Radiation

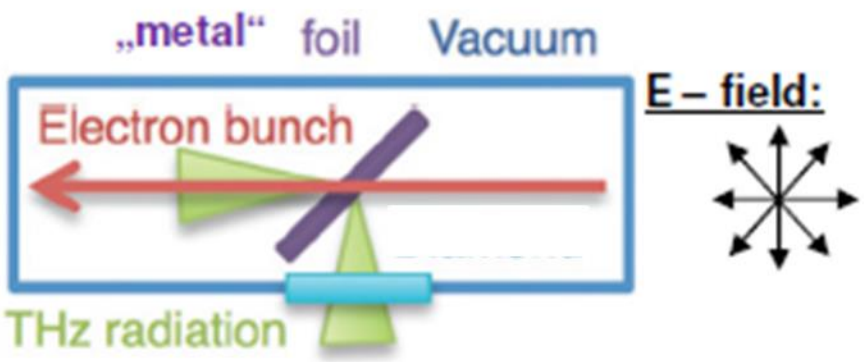

Undulator Radiation

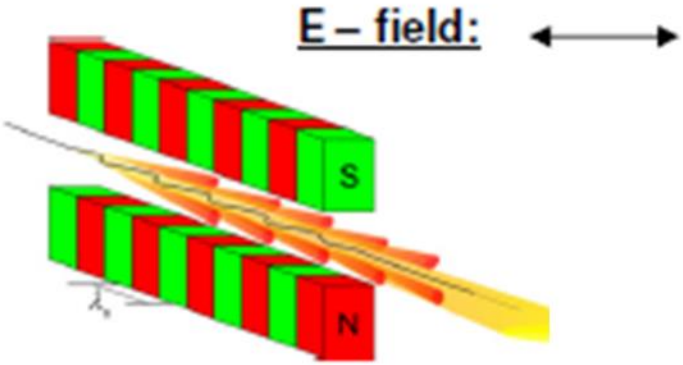

SPARC LAB: Linear accelerator at 250 MeV

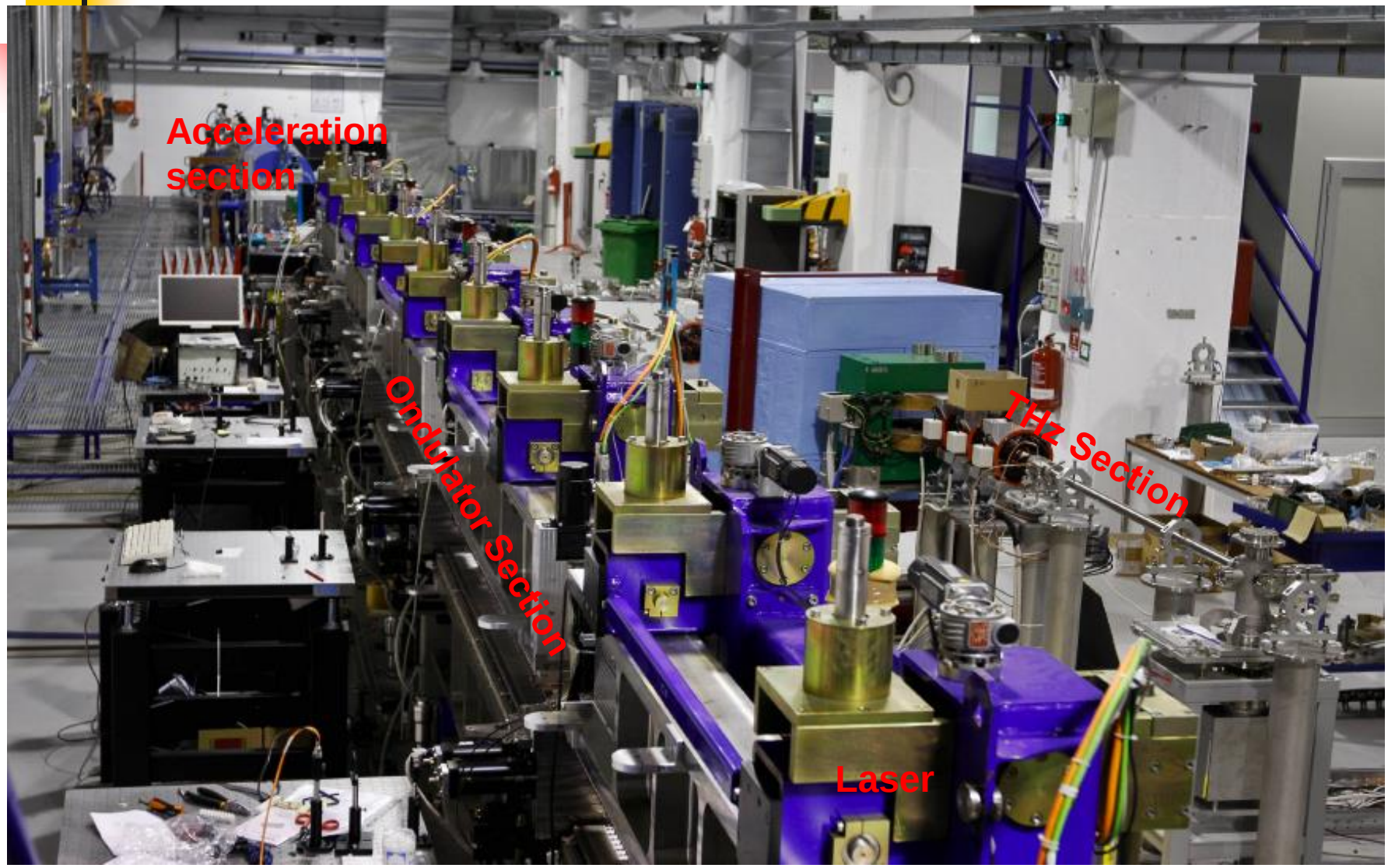

Achieved THz Performances

Electron beam parameters	Single bunch (VB mode: max compression)	4-bunches per train (VB mode + laser comb)
Charge/bunch (pC)	300	50
Energy (MeV)	130	100
Bunch length (fs)	160	200
Rep. Rate (Hz)	10	

Radiation parameters	SPARC (single bunch)	SPARC (4-bunches/train)
Energy per pulse (μJ)	40	0.6 10^{-6} (@ 1 THz)
Peak power (MW)	> 100	3 (@ 1 THz)
Electric field (MV/cm)	1.5	> 10
Pulse duration (fs)	120	< 100
Bandwidth	50 GHz-5 THz	50 GHz-5 THz

E.Chiadroni et al, APL 2013

3D Topological Insulators

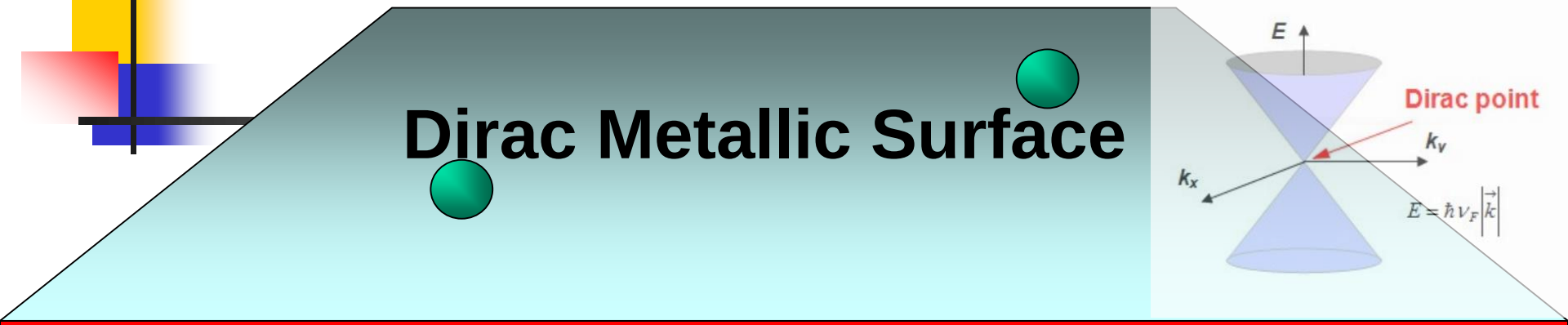

Insulating state in the bulk due to Spin-Orbit

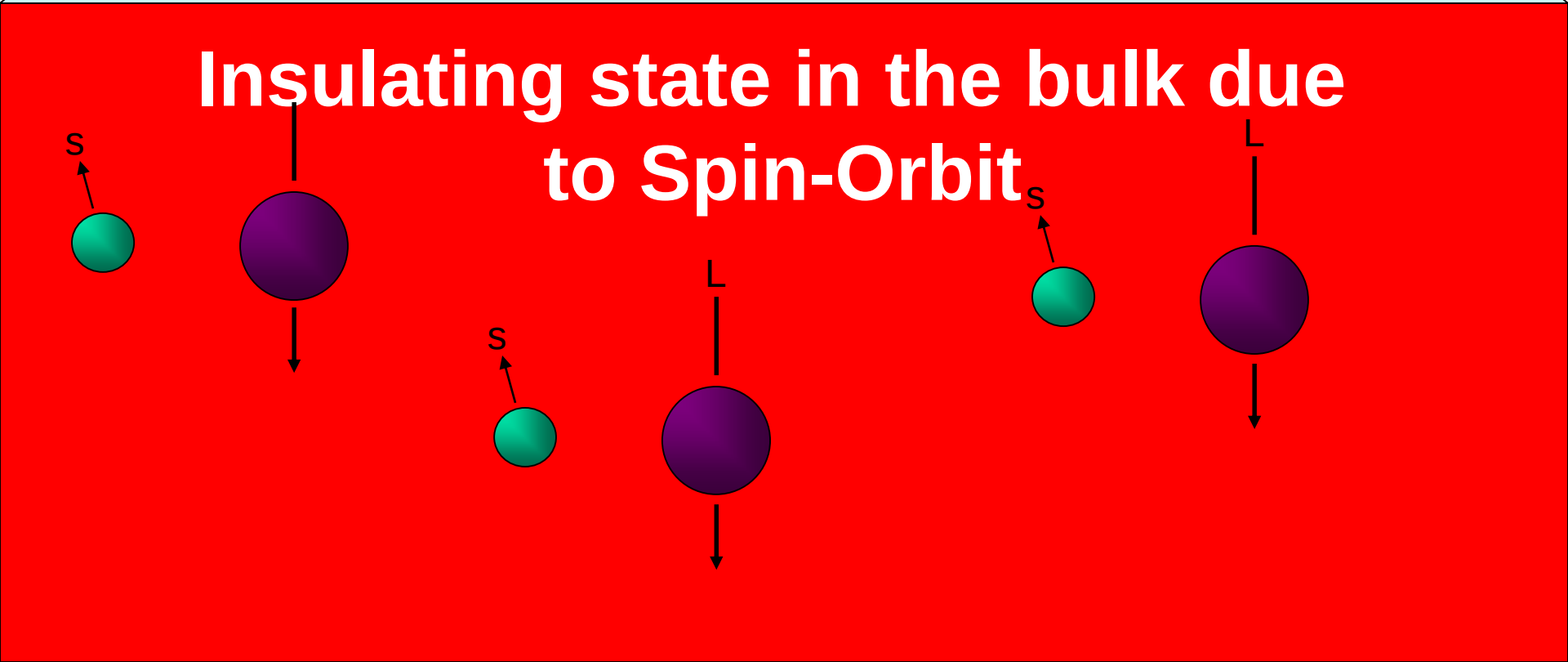

Non-Linear THz response of TI Dirac Fermions

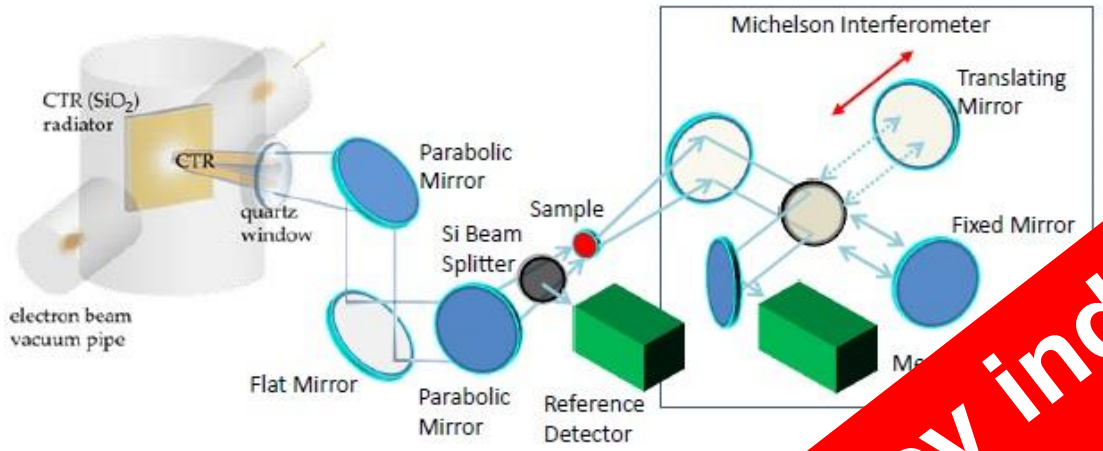

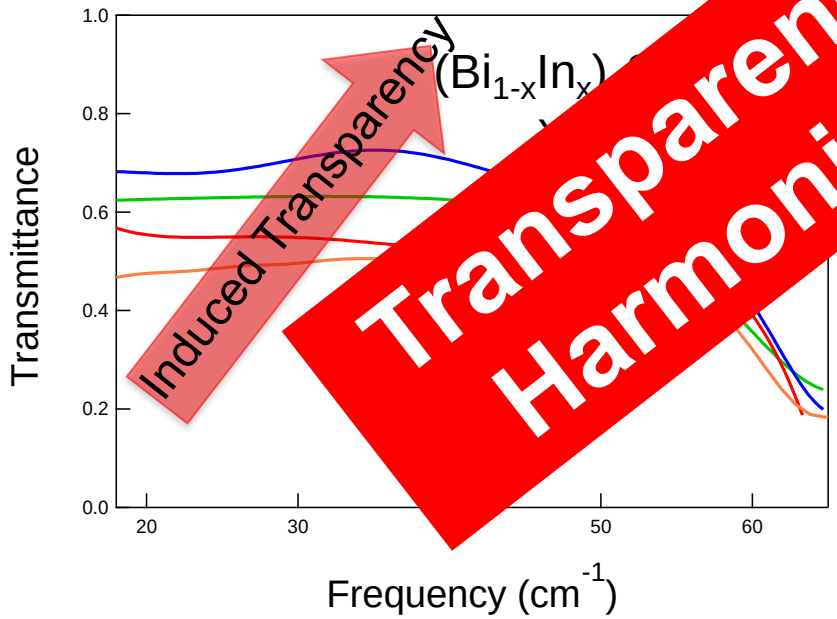

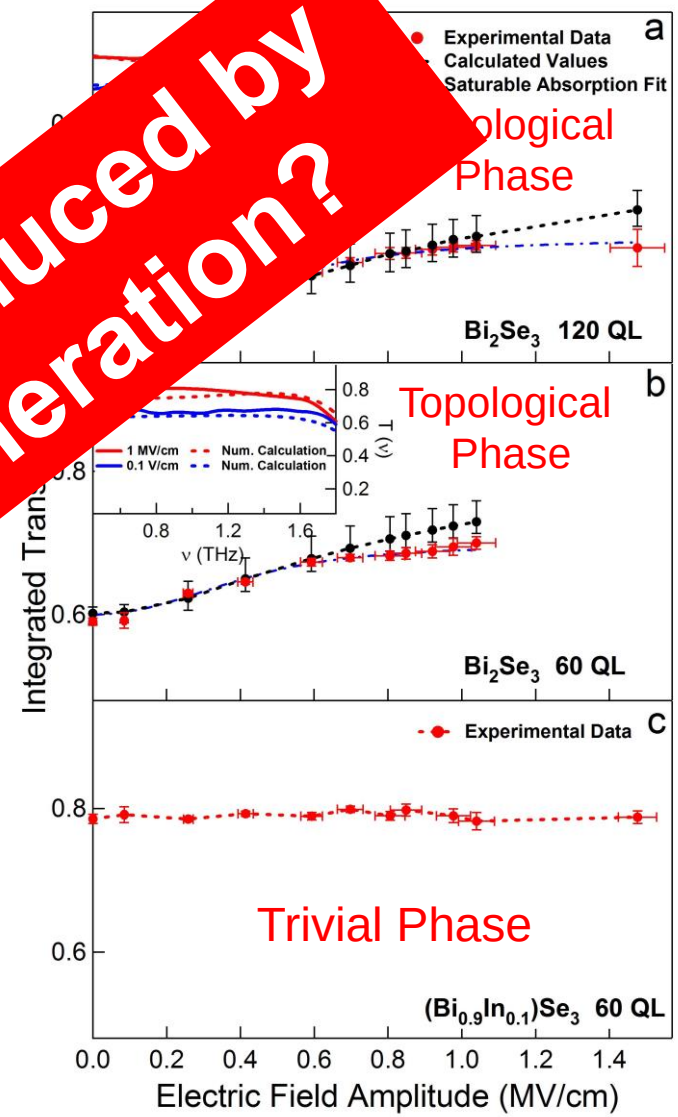

Transparency induced by Harmonic Generation?

F. Giorgianni et al., Nature Communications (2016)

Non-Linear THz response of TI Dirac carriers

According to the classical equation of motion one electron in an electric field **E** is accelerated with a momentum variation d**p**/dt=-e**E.** $\mathbf{E}=\mathbf{E}_0\cos\omega t \rightarrow \mathbf{p}=(-e\mathbf{E}_0/\omega)\sin\omega t$

Massive Electrons

$$\varepsilon(p)=\frac{\vec{p}^2}{2m}$$

$$\mathrm{v_x}=\frac{d\varepsilon}{dp_x}=\frac{p_x}{m}=\frac{-eE_0}{m\omega}\sin\omega t$$

For n electrons one has an electric current

$$J_x(t)=-en\mathrm{v_x}=\frac{\mathrm{ne}^2E_0}{m\omega}\sin\omega t$$

Linear current vs. E

Dirac Electrons

$$\varepsilon(p)=\mathrm{v_F}\sqrt{p_x^2+p_y^2}$$

$$\mathrm{v_x}=\frac{d\varepsilon}{dp_x}=\frac{\mathrm{v_F}p_x}{\sqrt{p_x^2+p_y^2}}=-\mathrm{v_F}\,\mathrm{sgn}\,\omega t$$

For n electrons one has an electric current

$$J_x(t)=-en\mathrm{v_x}(\mathrm{t})$$

$$=\mathrm{e}^2\mathrm{nv_F}\frac{4}{\pi}[\sin\omega t+\frac{1}{3}\sin 3\omega t+\ldots]$$

Unlinear current vs. E

Dirac THz Non-Linearity in Bi_2Se_3 Topological Insulator

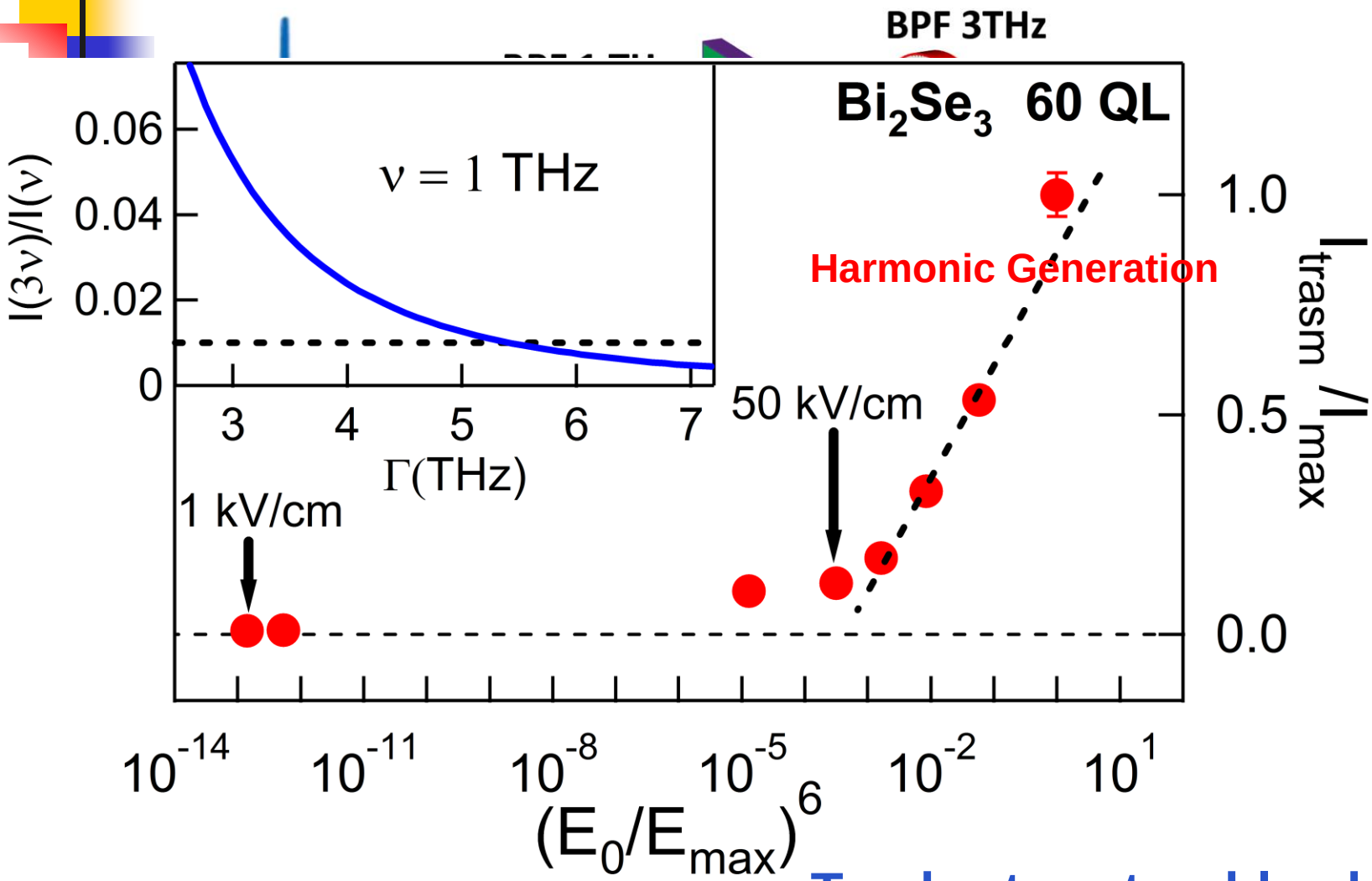

Terahertz saturable absorber

F. Giorgianni et al., Nature Communications (2016)

Go beyond the Diffraction Limit→IRSR Nanoscopy

The resolving capability of an optical component is ultimately limited by the diffraction (Abbe's theory, 1873). The minimum resolution (δ) for the optical component are thus limited by its aperture size, and expressed by:

$$\delta = 0.61\frac{\lambda}{NA} \approx \lambda$$

With a 36x objective with NA=0.5, one obtains:

at λ = 10 μm (1000 cm^{-1}):12 μm

DIFFRACTION LIMIT

at λ = 2.5 μm (4000 cm^{-1}):3 μm

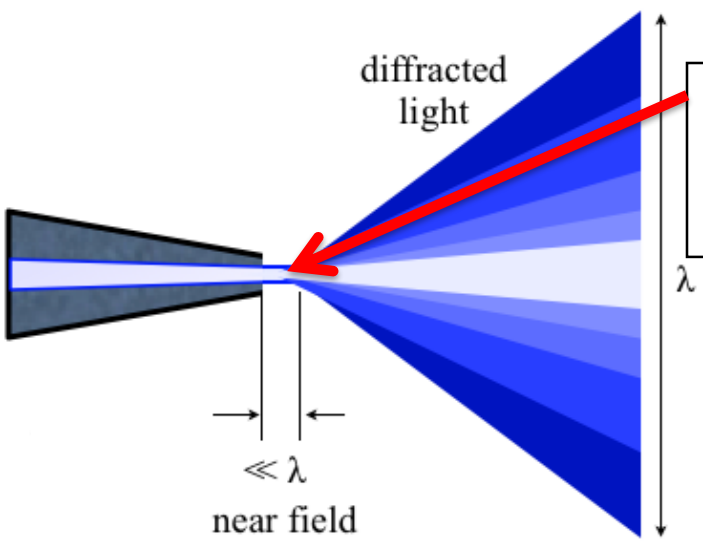

The fine spatial structure is contained in the near-field which exponentially decreases far from the focal point

Need to capture the near-field signal

Beyond the Diffraction Limit: The use of Evanescent waves

In order to enhance the spatial resolution one should increase the wavevector (k_x) bandwidth Δk_x :

For propagating ligth the ultimate limit of k_x=k$= 2\pi/\lambda$

Being k=$\sqrt{k_x{}^2 + k_y{}^2 + kz^2}$, k_x>>k$= 2\pi/\lambda$ if k_z is immaginary

An evanescent wave (along a direction) has along this direction an esponentially decreasing amplitude:

$$E(\mathrm{r,t})=\mathrm{E}_0 e^{ik_x x} e^{ik_y y} e^{-kzz}$$

Due to the evanescent nature, this wave which maximizes the spatial resolution should be analyzed at distances on the order of $k_z^{-1}\approx\lambda$ from the source

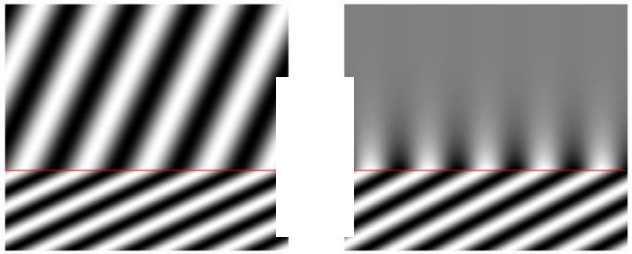

Generating and Capturing the Evanescent Waves

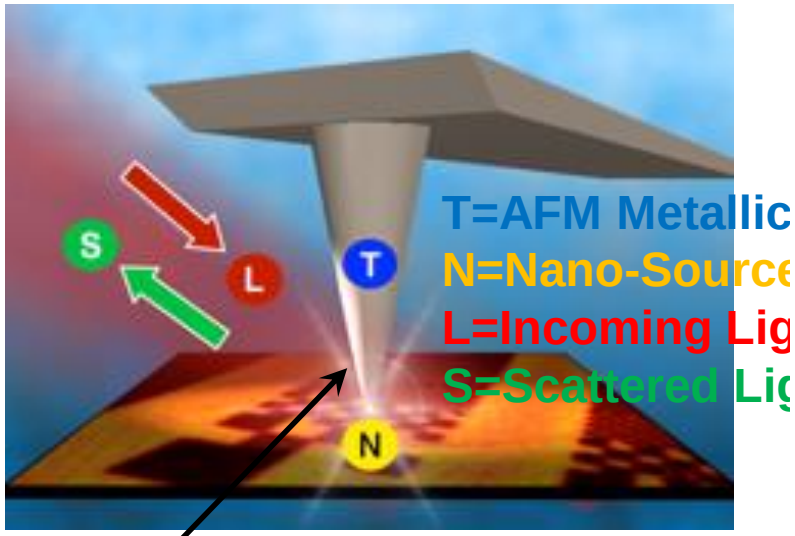

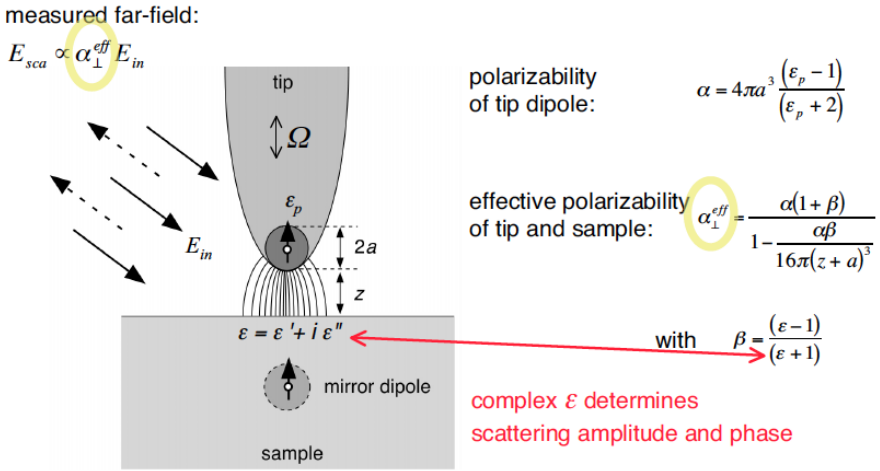

B. Knoll and F. Keilmann, Nature **399**, 134 (1999)

The metallic AFM-Tip acts as an antenna transforming far-field ligth in a plasmon which propagates to the apex localizing *em* energy on nanoscale dimension comparable to apex-size.

Spatial resolution ~ AFM tip radius

SPATIAL RESOLUTION INDEPENDENT OF λ

Comparison among different Spatially Resolved Spectroscopies

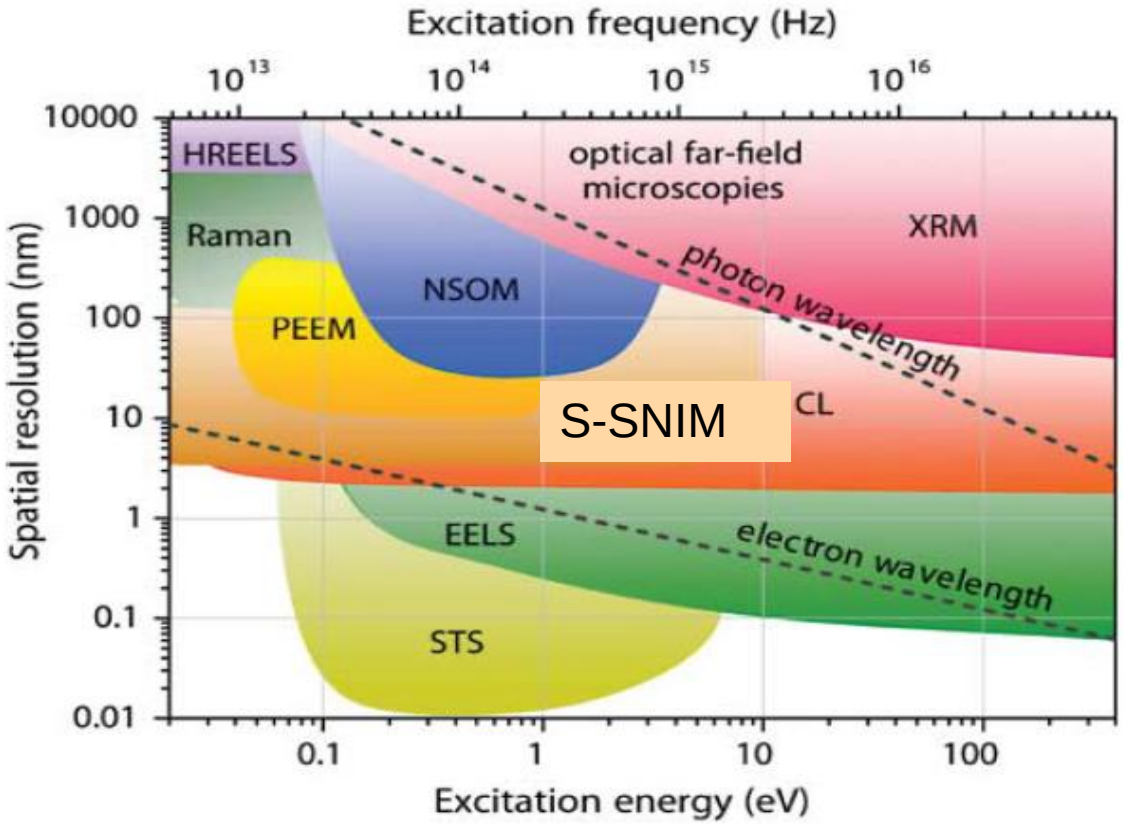

X. F. De Abajo 2010

Visualizing Plasmon Propagation and Scattering in Single Carbon Nanotube (Optics at Finite q)

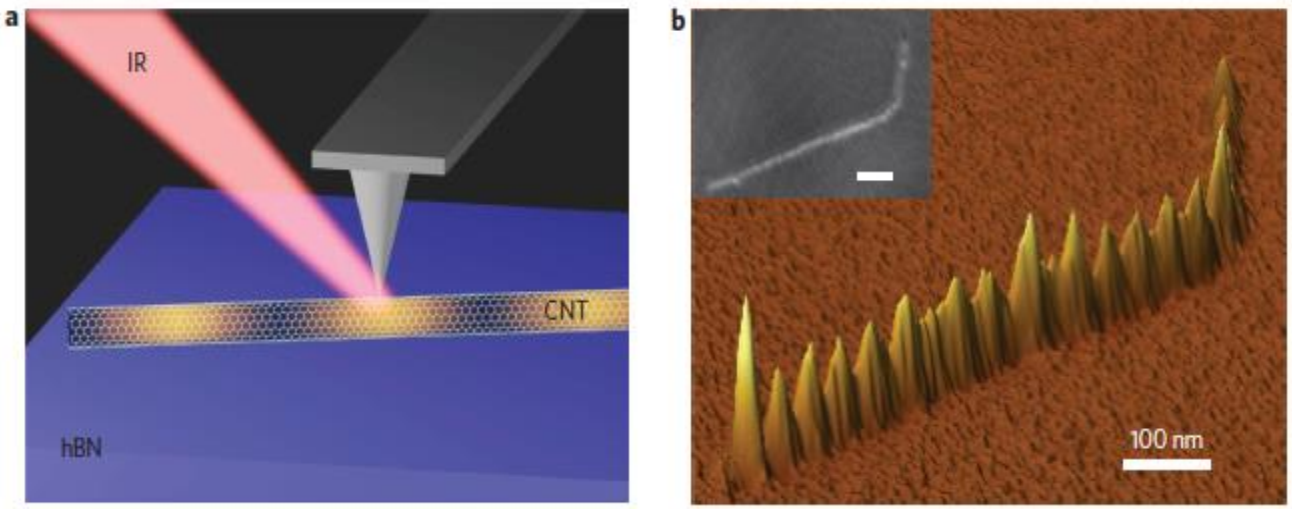

Figure 1 | Infrared s-SNOM of one-dimensional plasmons in carbon nanotubes. a, Illustration of s-SNOM. Infrared (IR) light is focused onto the apex of a metal-coated AFM tip, the large near-field momentum of which enables optical excitation of plasmons in the carbon nanotube (CNT) on a hBN substrate. Interference between the tip-excited plasmon wave and its reflection from the nanotube end leads to periodic modulation of tip-scattered infrared radiation measured by an HgCdTe detector in the far field. **b**, Three-dimensional plot of the near-field scattering intensity (height) along a representative SWNT. Prominent modulation of the infrared scattering intensity from the one-dimensional plasmon can be observed over the whole nanotube. Inset: AFM topography image of the same SWNT. Scale bars, 100 nm.

Z. Shi, Nature Photonics 2015, **IRSR from ALS IR Beamline**

Acknowledgments

The TERALAB group:
M. Daniele
L. Tenuzzo

FREQUENCY AND TIME-RESOLVED
TERAHERTZ SPECTROSCOPY

The SISSI/TERAFERMI-ELETTRA group:
A. Perucchi
P. Di Pietro
L. Vaccari

The LNF-INFN SPARC Lab group:
E. Chiadroni